Applied Intelligence (2020) 50:1112–1132
https://doi.org/10.1007/s10489-019-01551-z

A hybrid fuzzy filtering - fuzzy thresholding technique for region of interest detection in noisy images

Sanmoy Bandyopadhyay[1] · Saurabh Das[1] · Abhirup Datta[1]

Published online: 18 December 2019

Abstract
Noise leads to the ambiguity in regions of interest detection by corrupting the pixel information and is a vital problem in image processing domain. A novel hybrid technique based on fuzzy filtering and fuzzy thresholding is proposed here to extract the object regions accurately in presence of Gaussian noises. The proposed method is automated, does not need any parameter tuning as well does not need prior knowledge of the image or noise. An asymmetrical triangular fuzzy filter with median center coupled with a thresholding based on fuzziness minimization technique are implemented for this purpose. The fuzzy thresholding technique helps to classify the pixels with low signal-to-noise ratio (SNR) caused either due to noise or by the application of noise removal process. The proposed technique is applied in benchmark images corrupted by noises and are compared with some of the popular algorithms of object detection. The results indicate that the proposed method has superior performance in terms of peak signal-to-noise ratio (PSNR) and mean square error (MSE) value for images corrupted with Gaussian noises with standard deviation upto 1.5.

Keywords Region of interest detection · Gaussian noise · Fuzzy thresholding · Fuzzy filtering · Asymmetrical triangular function

1 Introduction

Detection and extraction of the object of interest (OoI) or region of interest (RoI) from images are challenging tasks, especially in the presence of noise. The complexity of the problem gets increased while dealing with natural or remote sensing images because of the presence of noise. The images are mostly encountered with Gaussian noise, salt and pepper or impulse noise, speckle noise, Poisson noise, and structured noise. The existence of noise distorts the actual image information by introducing additional unwanted signals in the image. This leads to blurring of the object, and vagueness in the corners and edges of the object. In general, the problem becomes all the more complicated as real images are usually in gray-scale, and the difference between object and background is very small, which often gets mixed-up due to the presence of noise.

There exists two broad methodologies for segmenting out RoI from the region of the images encountered with low signal-to-noise ratio (SNR). One method is through implementation of the segmentation technique directly on the noisy images, while the other is to pre-process the image and then implement the segmentation algorithm [24]. Some of the most popular techniques are threshold based segmentation [47, 51], clustering based segmentation [17, 23], fuzzy clustering based technique [57], region based methods [42], Neural Network based method [1], grow cut based segmentation [19], active contour model [61], watershed model [11], Markov Random Field (MRF) model [5], etc. In the recent past, few more techniques, such as Chan-Vese active contour model [22, 43], Fuzzy energy based active contour model [36], two-dimension (2D) Otsu's thresholding [30], and superpixel based segmentation method [31, 39] have been developed for the segmentation purpose. Among these, most are not suited for segmentation of noisy images, while some are robust to the noisy

✉ Saurabh Das
das.saurabh01@gmail.com

Sanmoy Bandyopadhyay
sanmoy1985@rediffmail.com

Abhirup Datta
abhirup.datta@iiti.ac.in

[1] Discipline of Astronomy, Astrophysics and Space Engineering, Indian Institute of Technology, Indore, Simrol, Indore 453552, India

environment [48]. Moreover, these methods are capable of producing the desire output only for high values of SNR [24].

There exists various state-of-the-art methodologies for segmenting out RoI from low SNR images by applying de-noising followed by segmentation algorithm[4, 24, 45]. Some of these techniques are a combination of; bilateral filter, superimposing technique and Otsu's thresholding [45], average filtering and gradient based thresholding [44], double mean filtering and Otsu's thresholding [46], guided filter and fuzzy clustering [24], etc. For de-noising purposes, Gaussian filter [16], Kalman filter [12], Wiener filter [6], averaging filter technique [50, 51], and median filter [21] are being widely used. Recent techniques like, artificial neural network based methods [18, 58], fuzzy based methods [38], clustering based techniques [15] and wavelet transform [6] have also been proposed for image de-noising. However, these noise removal methods sometimes lead to vital information loss during image pre-processing step [24].

The majority of the existing methods require manual intervention either in parameter tuning or contour initialization. Some of the methods like machine learning based models also need prior training data sets. The aim of this paper is to introduce a hybrid method which is fully automated and does not require any prior knowledge. Here, we focus only on one type of noise, i.e. Gaussian noise which is one of the most commonly encountered noises in remote sensing images. The main reason behind the occurrence of this noise is the distortion in signal level during the transmission of data as well as the variation in illumination (https://homepages.inf.ed.ac.uk/rbf/HIPR2/noise.htm, www.nhu.edu.tw/~gshwang/ImageProcessing/Chap08.ppt). Here we propose a hybrid fuzzy based filtering and thresholding (FFFT) technique to handle the high Gaussian noise for image segmentation purpose in low SNR region. The fuzzy concept is introduced to handle the ambiguity of the pixels due to low SNR values. On the other hand, thesholding based technique has been used for its simplicity and time efficiency. The results of the proposed method has been compared with heuristic combination of various state-of-the-art de-noising methods and Otsu's or fuzzy thresholding, and recently developed image segmentation techniques. The main contributions of this article are:

- Integration of fuzzy theory simultaneously for both image de-noising and object detection tasks.
- The development of the fully automated FFFT technique for image segmentation in low SNR images.
- Establishment of heuristically combined method of different noise removal techniques and thresholding based segmentation technique.

The proposed technique has been tested on a few synthetic and real benchmark data sets, and the results have been compared with other existing techniques of image segmentation like 2D Otsu's thresholding [30], superpixel-based fast fuzzy C-means clustering (SFFCM) [39], modified Otsu-based image segmentation algorithm (OBISA) [59], Region-based active contour model driven by fuzzy c-means (RACMFCM) [32], and with heuristically integrated segmentation techniques (Otsu's/fuzzy thresholding) along with different noise filters such as; recursive filtering (RF) [10], statistical nearest-neighbor (SNN) method [20], super-resolution convolutional neural network technique (SRCNN) [18], Gaussian/bilateral filtering and method noise thresholding (G/BFMT) [53], guided filter and fuzzy clustering (GF-FCM) [24].

The overall flow of the paper is as follows: the related work on noise removal and object detection have been discussed in Section 2 of this paper. Section 3 discusses the proposed techniques. Results and discussions have been given in Section 4. Section 5 provides the overall conclusion and future scope of the work.

2 Related work on object detection in noisy image

The methods associated with noisy image segmentation can be broadly classified into two groups namely; noise removal in pre-processing followed by segmentation and direct segmentation techniques. A brief detail of these processes are outlined in the following subsections.

2.1 Noise removal techniques

Gaussian filtering based image de-noising [16] is widely used for the removal of Gaussian noise. The filtering algorithm involves convolution operation. Here the convolution operation is performed directly between the image pixel and Gaussian function, as a output de-noised image is obtained. The filter perform like a low pass filter while performing the noise removal operation. During the process their is a chance that most of the noisy pixels remained in the image after the first convolution operation of the image with that of the Gaussian function [41].

In order to overcome this limitation of classical Gaussian filter, an iterative Gaussian filtering had been induced for the scale invariant feature transform (SIFT) purpose [41]. In this iterative filtering operation the resultant image obtained from the Gaussian filtering operation is again pass through the convolution operation using the Gaussian function for certain number of iteration repetitively. In-spite of several

advantages, Gaussian based filtering technique has few drawbacks. The filter blurs out (degrade the resolution) the image in order to reduce the effect of noise. Additionally, it often vanishes the edge information as well give rises to the phantom edge [16]. Moreover, the performance of Gaussian filter depends on the value of variance (σ) used in Gaussian function and the determination of σ value requires a supervised approach. Human supervision is also needed for the determination of numbers of iteration for performing iterative filtering operation.

Gaussian/bilateral filtering and method noise thresholding (G/BFMT) using wavelets had been proposed by Kumar [53] in-order to handle the drawback of classical Gaussian or bilateral filter of noise removal. The bilateral filter can store the edge information, but often remove some image details. In order to restore the image details from the method noise, Kumar [53] had introduced wavelet thresholding technique, where method noise had been transformed into wavelet domain. The accuracy of the method also depends on proper selection of noise variance.

Mean filter [50] is another filter for such purpose, but perform very poorly when there is a huge variation of pixel values present in the window under consideration.

Kalman filter based on recursive algorithm is also used for image de-noising. The filter is an optimal estimator and has the capability to handle all the uncertainties related with noisy image. Parameter setting is a critical issue in Kalman filter based technique[12]. The outcome varies widely if the input parameters given are not adequate.

The fast and robust recursive filter (RF) had been used for the image de-noising in order to reduce the complexity of the noise removal algorithm [10]. In this method, the de-noised output from modified 1st-order and 3rd-order recursive filter (RF) had been fused based on Stein's Unbiased Risk Estimator (SURE) [54]. The outcome from recursive filter based de-noising method had been compared with the results of BM3D [13], Non-Local-Means (NLM) [7], 1st-order-RF and 3rd-order-RF. Although the method outperform in terms of peak signal-to-noise ratio (PSNR), but it is having longer run-time [10]. A statistical approach based wiener filter has also been proposed for image de-noising [37]. The filter use the parameters like mean, standard deviation for noise detection and removing. This filter also smooth out the image, which in turn results in information loss of the image.

Traditional Non-Local-Means (NLM) of image de-noising algorithm involve three vital steps for removing noise from the image [8, 20]. These are, identification of neighbors for each patch, averaging neighbors and aggregation of de-noised patches [20]. In order to reduce the error in prediction of noise free patch and to overcome the bias due to nearest-neighbors search strategy, Frosioand and Kautz [20] had introduced statistical nearest-neighbors (SNN) searching algorithm. The method aims in gathering neighbors which has squared distance close to its expectation with respect to the reference patch. An offset parameter used to force the algorithm to move from traditional nearest-neighbors to SNN based technique. The method leads to improvement of image quality also for the case of bilateral filtering, along-side the method is effective for the homogeneous region in an image [20]. The results from the technique had been compared with those of BM3D [13], BM3D-CFA [14], sliding discrete cosine transform filter (SDCT) [63] and traditional nearest-neighbors based algorithm.

Various version of the neural network (NN) based technique had also been used for removal of noise from the image. One of the most simpler versions of NN based de-noising technique had been implemented by Ohana (https://www.cs.bgu.ac.il/~ben-shahar/Teaching/Computational-Vision/StudentProjects/ICBV071/ICBV-2007-1-ArieOhana/index.php). The method introduced with single hidden layer along with input and output layers. The overall structure of the network 10-50-1. In the very first layer input from the pixel of the noisy image is feed into one neuron of the input layer, while the other neuron is feed with the pixel intensity from the same coordinate of the source image. Pixels intensity of 8 neighbors of the considered pixel is feed into rest of the neuron of the input layer. The weighted sum of the output received from the middle layer is being calculated in a single neuron present in the last layer of the network to generate the de-noised result. In the work, sigmoid function had been used. The method require additional supply of original image as a training set.

Turkmen [58] in recent past had introduced the artificial neural network based method for removal of random valued impulse noise from the image. The method showed its promising capability to remove noise compared to the other algorithms, but, require more computational time[58].

In super-resolution convolutional neural Network (SRCNN) a deep neural network (DNN) based algorithm had been implemented [18]. The method involves three main operational parts. These are patch extraction and representation, non-linear mapping and reconstruction. The overall performance of the CNN depends on the proper optimization of biases and filtering weight as-well-as on training strategies of the network. Sparse coding-based method [62], integrated neighbour embedding and locally linear embedding method [26], anchored neighbourhood

regression method [55], adjusted anchored neighbourhood regression method [56] and KK- the method [34], used for comparison with SRCNN.

Among fuzzy based noise removal techniques, the symmetrical triangular fuzzy filter with median center (TMED), Gaussian fuzzy filter with median center (GMED), Gaussian fuzzy filter with moving average center (GMAV), asymmetrical triangular fuzzy filter with median center (ATFFMED) [38], the symmetrical triangular fuzzy filter with moving average center (TMAV), decreasing weight fuzzy filter with moving average center (DWMAV), and asymmetrical triangular fuzzy filter with moving average center (ATMAV) had been implemented by Kwan [38]. These filters were found to be capable of handling Gaussian noise with a maximum variance of 0.106 [38].

Fuzzy filter had also been used by Peng and Lucke [49] for the removal of noise mixed with Gaussian noise as well as impulsive noise. Here in the work [49], the authors had used non-linear fuzzy filter for filtering purpose, However, the method is a supervised technique where fuzzy membership had been trained with local features for noise removal task.

Ville et al. [60] had also used fuzzy filter for noise removal. The authors in the paper [60] had implemented fuzzy derivative for additive noise filtering.

Recently, Median filter with decision based model has been used for filtering noise from highly affected images [33]. In the work FPGA set up and strives has been implemented in order to remove impulse noise from the image with less computation time. The method shows its promising results compared to the output obtained from standard median filtering (SMF) and adaptive median filtering (AMF).

2.2 Segmentation techniques

Otsu's thresholding based segmentation [47] is one of the popular methods. This technique aims to partition the image into foreground and background based on the maximization of inter-class variance. Although being one of the simplest image segmentation technique, it shows its limitation in segmentation for a low value of inter-class variance. Alongside, the method alone is not robust to noise.

Classical Otsu's thresholding method [47] does not consider the intensity values of the neighboring pixels [30]. 2D Otsu's thresholding was introduced by Jianzhuang et al. [30] in order to overcome the drawback of classical Otsu's thresholding based segmentation. The method used the concept of averaging filter, where the mean value of the neighborhood pixels has been taken along with the gray-level intensity values to calculate the thresholds. Another advantage of 2D Otsu's thresholding method is that the technique is capable of withstanding Gaussian noise.

A modified Otsu-based image segmentation algorithm (OBISA) had been introduced, which replace the variance formula with standard deviation for the computation of optimal threshold [59]. The method is capable to set reasonable threshold value by removing the outliers, but computationally-expensive compared to classical Otsu's method.

Recently, active contours driven by non-local Gaussian distribution fitting (NLGDF) energy had been proposed for image segmentation by Li et al. [40]. The model uses patch level information to describe each local image region. The model outperforms the local Gaussian distribution fitting (LGDF) model in segmenting images in presence of heavy noises. A level set formulation of the NLGDF energy had been used by representing the image regions. Then variational methods was incorporated to solve the energy minimization problem. Contour initialization is a major problem in this method. The contour needed to be initialize on the object in the image.

Global and local weighted signed pressure force (SPF) based active contour model had also been used for segmenting images [25]. Here, first, a new global weighted SPF (GWSPF) had been defined. Second, a new local weighted SPF (LWSPF) was introduced to the above global weighted SPF. Third, the local and global within-class variances of the image are used to weight the GWSPF and the LWSPF. The model is robust to the initial curve. However, it depends on the image gray-scale information to control the contour evolution.

A fractional order derivative based active contour model based segmentation had been introduced by Chen et al. [9]. The method incorporates image gradient, local environment and global information for this purpose. The Energy or level set functions in this method include both global term and local term. The global term aims to enhance the image contrast, while local term integrates fractional order differentiation. The model is robust to noisy image and capable for inhomogeneous image segmentation. However, it is not suitable for uneven illuminated image segmentation. In addition, the method suffer from the problem of parameters selection.

Fuzzy energy based active contour model for image segmentation [36] is one of the techniques which can directly be applied to noisy images. In this technique, the fuzzy membership values determine the object region in the image.

Region-based active contour model driven by fuzzy c-means (RACMFCM) energy had been implemented for fast image segmentation [32]. The method used fuzzy c-means energy to rapidly compute the two sorts of cluster center functions for all points in the image. These two functions are used to substitute the time-consuming local fitting functions in traditional models. Moreover, a Gaussian filtering and

a sign function are used to supplant the length term and the penalty term in most models, respectively. The model is robust to contour initialization and noise, and segment intensity inhomogeneous image with higher accuracy and faster rate. But, it is only applicable for segmenting two-phase images.

Classical fuzzy C-means clustering (FCM) [3] aims in segmenting the image by minimizing the objective function. Despite several advantages, the method is very sensitive to noise as the neighborhood pixel information is not taken into account while segmenting an image. Moreover, the FCM algorithm has a high computational complexity, since it calculates the distance between clusters center and each of the pixels present in the image [39].

In order to overcome the mentioned drawback of FCM, Lei et al. [39] had introduced SFFCM for image segmentation. The method reduces the complexity of FCM by considering histogram of superpixel images, which is quite less in number as compared to a number of pixels present in the image. The superpixel images had been obtained using the watershed transform based on multiscale morphological gradient reconstruction (MMGR-WT) [39]. The algorithm is suitable for fast segmentation of color image, but it require prior information about the cluster number like other k-means clustering algorithms, for practical applications.

Recently Jin [31] had proposed a super pixel segmentation method for removal of impulse noise from a color image. A recursive vector median filter with adaptive window sizes had been taken into account for the task of object detection in the noisy image [31].

Zho et al., [64] had introduced multiobjective evolutionary clustering based image segmentation algorithm for segmentation of noisy image. The work used a noise robust IFS (NR-IFS) followed by a novel noise robust multiobjective evolutionary intuitionistic fuzzy clustering algorithm (NR-MOEIFC). In the work, firstly a three-parameter intuitionistic fuzzy distance measure is computed and secondly intuitionistic fuzzy fitness functions is constructed. Then a nonuniform intuitionistic fuzzy mutation operator is developed for generation of an intuitionistic fuzzy cluster validity index. This is then used to select the optimized solution from the final non dominated solution set [64]. The method outperform other state-of-the-art methods in noise robustness and computational time. However, finding of the exact Pareto optimal solution and the cluster number is the major limitation of this method.

Modified moth-flame based optimization algorithm had been also used for the multilevel thresholding segmentation of an image by Jia et al. [28]. The method involve two innovative strategies to segment an image. On one hand, self-adaptive inertia weight scheme is used for enhancing both exploitation and exploration, on the other hand, a heuristic thresholding (TH) is incorporated into moth-flame optimization (MFO) to improve the overall performance of multilevel thresholding. Otsu's variance, and Kapur's entropy criteria are employed as fitness functions to find the optimal threshold values of an image. The method has outperformed in terms of stability, efficiency, accuracy, and convergence rate.

Another hybrid multiverse optimization algorithm with gravitational search (GSMVO) algorithm had been

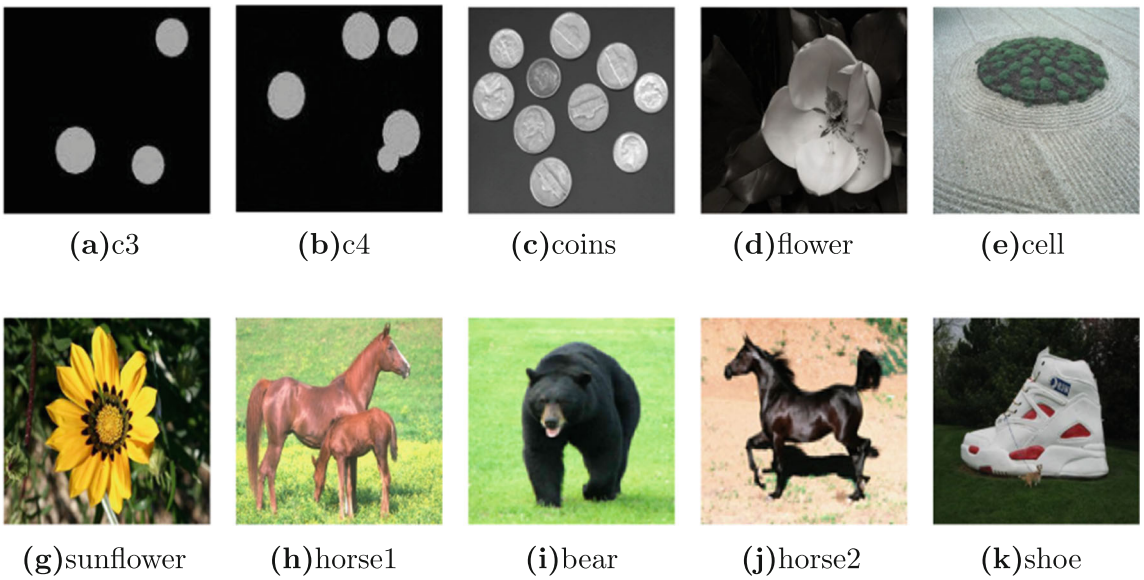

Fig. 1 Datasets used for the experiment. Caption of the images indicate the image name

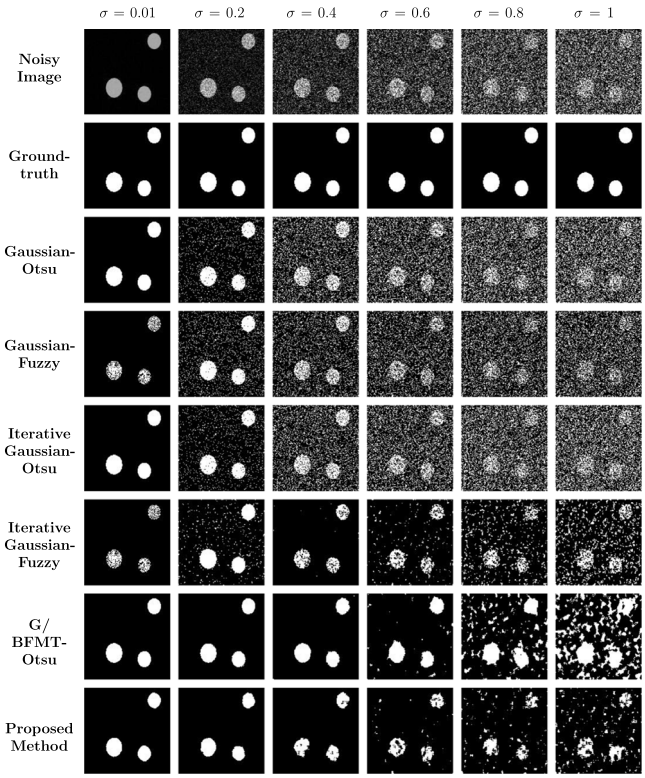

Fig. 2 Visual comparison between Gaussian based methods and proposed method for image *c3*

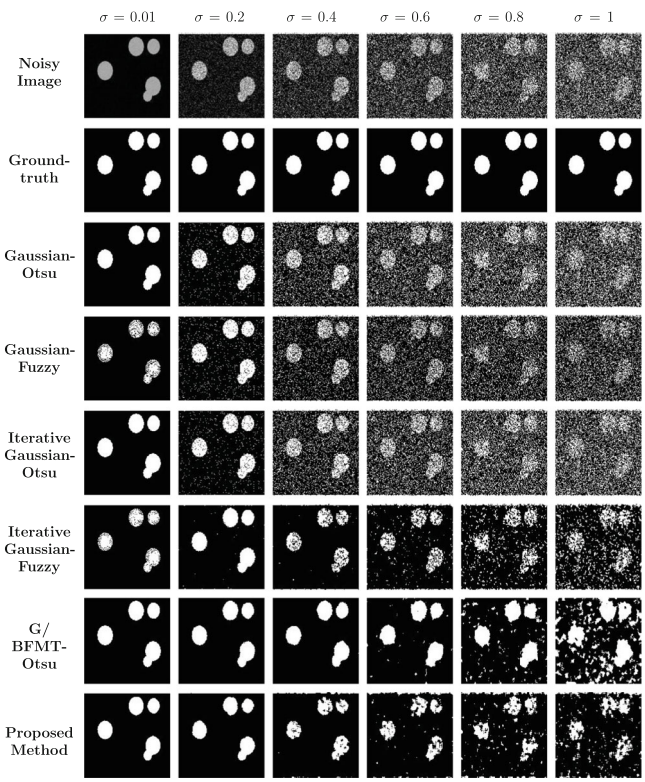

Fig. 3 Visual comparison between Gaussian based methods and proposed method for image *c4*

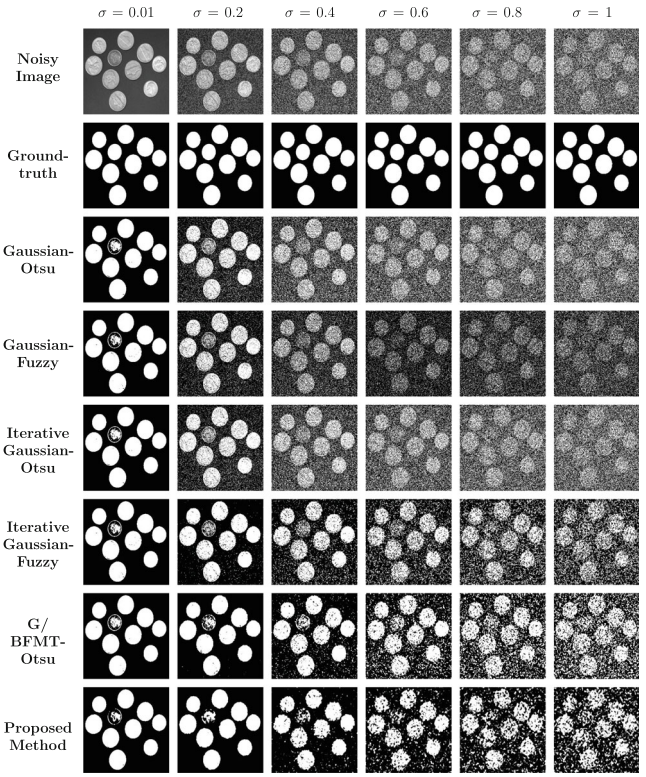

Fig. 4 Visual comparison between Gaussian based methods and proposed method for image *coins*

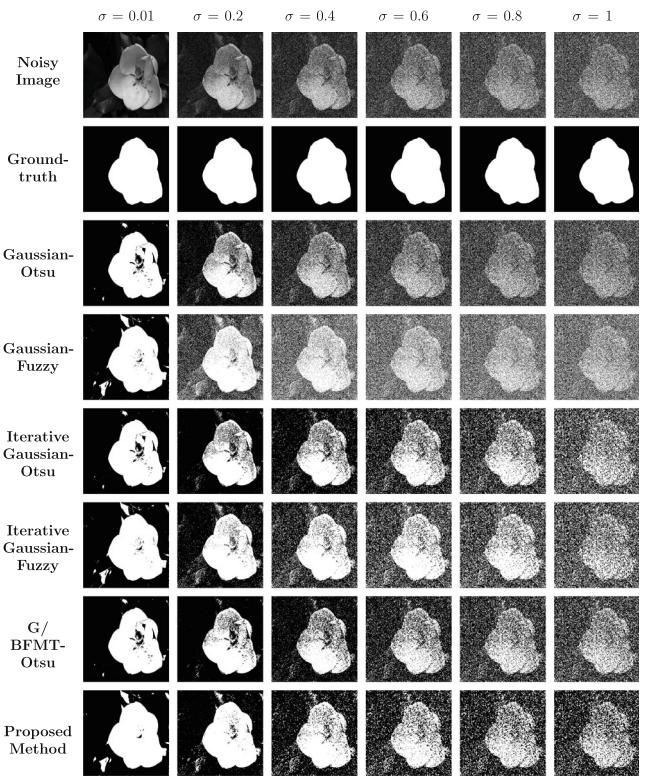

Fig. 5 Visual comparison between Gaussian based methods and proposed method for image *flower*

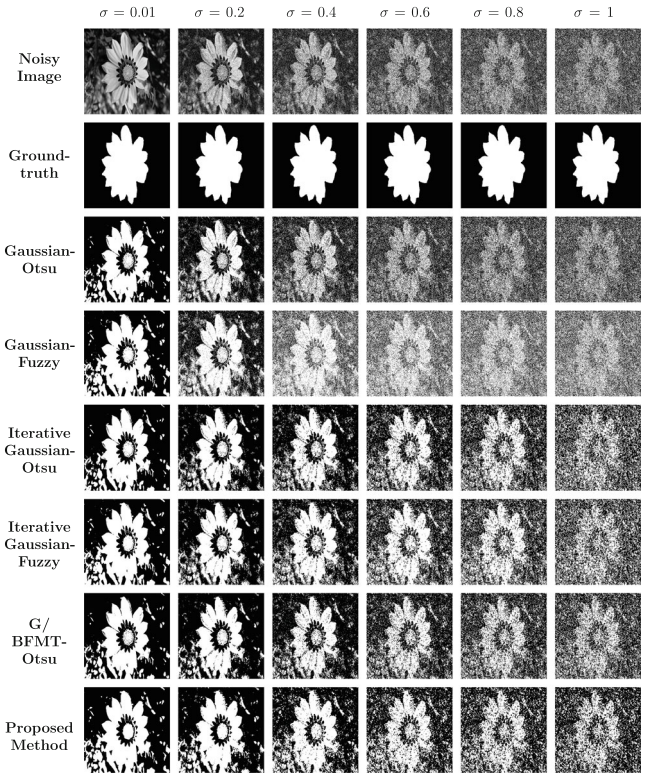

Fig. 6 Visual comparison between Gaussian based methods and proposed method for image *sunflower*

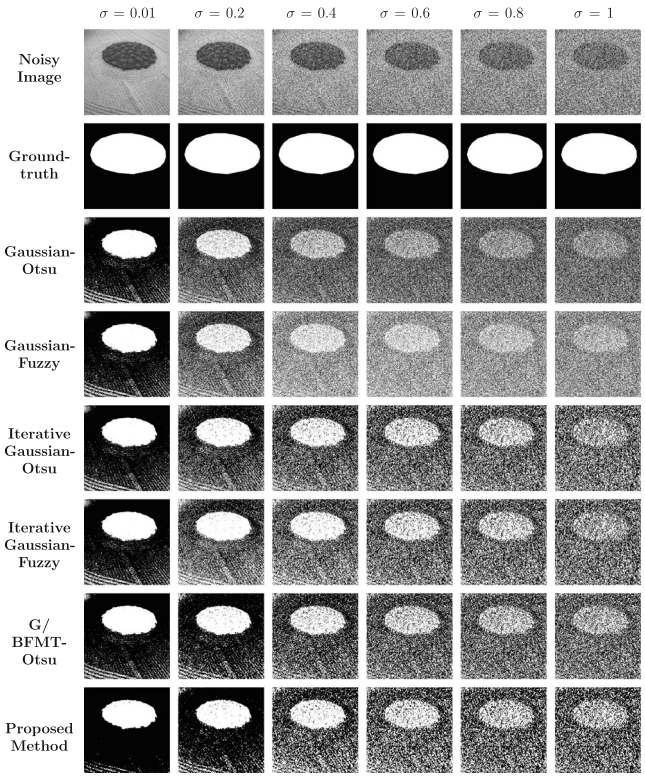

Fig. 7 Visual comparison between Gaussian based methods and proposed method for image *cell*

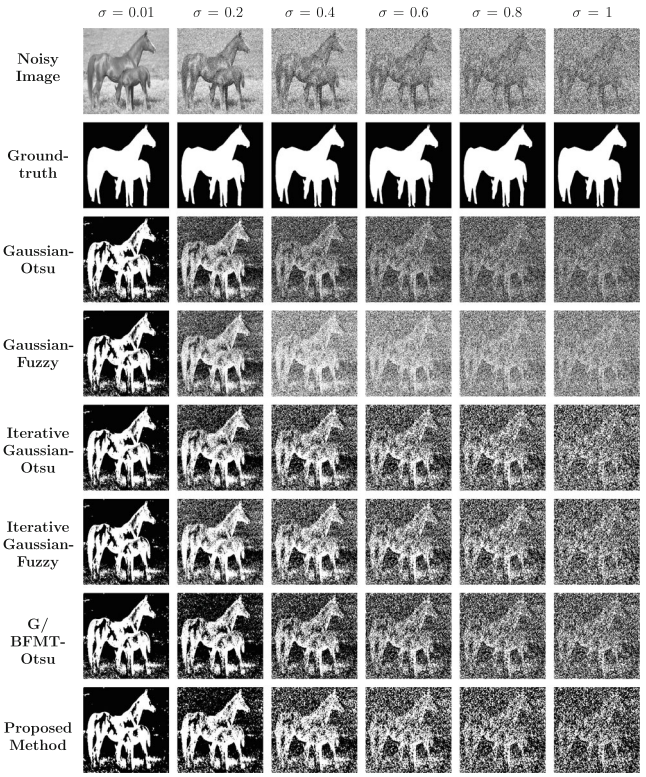

Fig. 8 Visual comparison between Gaussian based methods and proposed method for image *horse1*

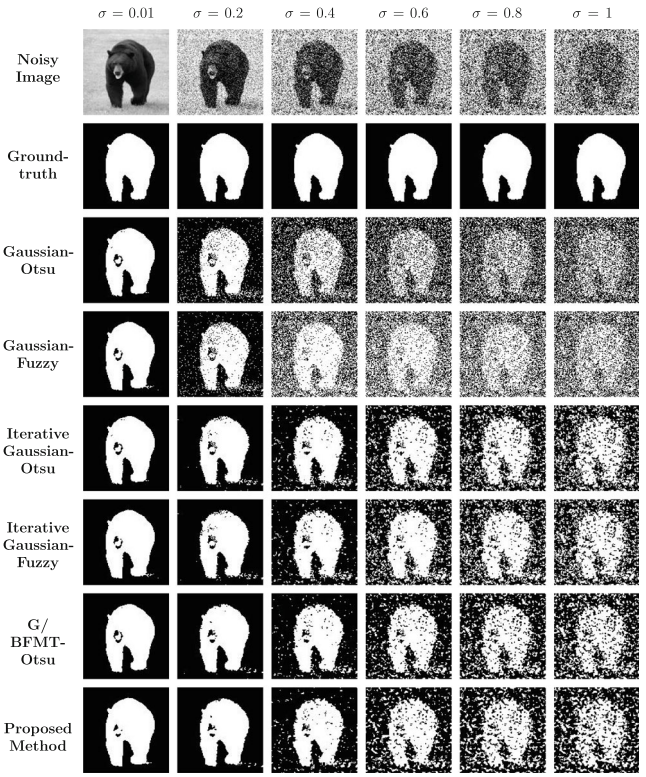

Fig. 9 Visual comparison between Gaussian based methods and proposed method for image *bear*

implemented for image segmentation [29]. It also takes the Otsu or Kapur's entropy as the objective function to find the optimal threshold of image segmentation. It shows better robustness on noise for large value of PSNR in cost of time complexity.

3 Proposed FFFT technique for object detection

In this work a hybrid fuzzy filtering and fuzzy thresholding (FFFT) based methodology has been proposed. The technique has been implemented in order to segment the noisy image withstanding the blurring effect caused by the filtering techniques. The technique works in two steps, first fuzzy filtering technique is used for generating the de-noised image and, next the segmentation task is done on the de-noised image using a fuzzy thresholding method. An asymmetrical triangular fuzzy filter with median center (ATFFMED) has been used for removing noise from the image [38].

The asymmetrical triangular fuzzy filter with median center (ATFFMED) filter compromise of a hybrid combination of median noise filter with the notion of fuzzy logic. The median filter is a non-linear filter, which carry forward the task of image de-noising in two steps [52]. In the first step, the filter carry out clustering function, where it performs the clustering of corrupted and non-corrupted pixels. After the clustering, in the second step, the filter pass through the noisy pixels and restrain uncorrupted pixels in the image. These corrupted pixels are being removed from the image based on the median value. The overall formulation of the classical median filter is given by;

$$J(x, y) = median\{I(x - p, y - q) \mid (p, q) \in W\}. \quad (1)$$

In (1), J and I are the output (de-noised) and the input (noisy) images, where x and y are their spatial co-ordinates along x and y axis respectively. The term W represents the filtering window (square window) of size $K \times K$ and length $Len = 2K + 1$, with it center co-ordinates at (p, q).

The main advantage of the median filter is to retain the edge information while filtering out the noisy pixels present in the image [52], however, often eliminates corners and thin lines [35]. Moreover, it generates undesired results for signal dependent noises [35]. In order to preserve the fine structure in the image and to handle the vagueness associated with the classification of the noisy pixel, the fuzzy concept had been introduced [52]. Where the median value has been determined based on the value of the center pixel of the window. The output value of the fuzzy based median filter is estimated by;

$$J(x, y) = \frac{\sum_{(p,q)\in W} \mu(x + p, y + q).I(x + p, y + q)}{\sum_{(p,q)\in W} \mu(x + p, y + q)}. \quad (2)$$

The term μ represents fuzzy membership values, where the asymmetrical triangular function is considered to represent the membership values. The membership value μ is calculated as given in (3):

$$\mu(x, y) = \begin{cases} 1 - \frac{I_{med}(x,y) - I(x+p,y+q)}{I_{med}(x,y) - I_{min}(x,y)} \\ \quad \text{for } I_{min}(x, y) \le I(x + p, y + q) \le I_{med}(x, y) \\ 1 - \frac{I(x+p,y+q) - I_{med}(x,y)}{I_{max}(x,y) - I_{med}(x,y)} \\ \quad \text{for } I_{med}(x, y) \le I(x + p, y + q) \le I_{max}(x, y) \\ 1 \quad \text{for } I_{med}(x, y) - I_{min}(x, y) = 0 \\ \quad \text{or } I_{max}(x, y) - I_{med}(x, y) = 0. \end{cases} \quad (3)$$

Where, the terms $I_{med}(x, y)$, $I_{min}(x, y)$ and $I_{max}(x, y)$ represent the median, minimum and maximum value of intensity present in the particular window of the filter for input of $I(x+p, y+q)$. The asymmetric triangular function has the advantage of reduction in fuzziness and increased accuracy level of decision making or prediction [2].

The advantage of image segmentation based on fuzzy thresholding is that it can handle the problem associated with the overlapping of two classes which are often encountered in de-noised images. Particularly, the pixels near object boundaries often become ambiguous during the de-noising process. In the present work, fuzzy thresholding technique, proposed by Huang and Wang [27], has been used for its simplicity and less computational time requirement.

The threshold value has been estimated based on the optimization function for de-noised image J of size $M \times N$ and had been defined as:

$$E(T) = -\frac{1}{MNln2} \sum_{x=0}^{M-1} \sum_{y=0}^{N-1} S_e(\mu_J(J(x, y))), \quad (4)$$

where S_e represents Shannon's entropy function (5).

$$S_e = -\mu_J ln\mu_J - (1 - \mu_J)ln(1 - \mu_J). \quad (5)$$

The entropy function had been used as a cost function, which decreases as the fuzziness of the image pixels

reduces. The term μ_J in (4) and (5) denotes the membership function which is given by;

$$\mu_J(J(x,y)) = \begin{cases} \dfrac{1}{1-|J(x,y)-m_1(T)|/D} & \text{if } J(x,y) \le T \\ \dfrac{1}{1-|J(x,y)-m_2(T)|/D} & \text{if } J(x,y) > T. \end{cases} \tag{6}$$

In the (6) D is a constant which is given by,

$$D = J_{max}(x,y) - J_{min}(x,y); \tag{7}$$

where $J_{max}(x,y)$ and $J_{min}(x,y)$ are the maximum and minimum gray levels intensity present in the de-noised image respectively. And the terms m_1 and m_2 are the average gray level pixels present in two classes determined based on the initial threshold value T. The terms m_1 and m_2 are denoted as;

$$m_1 = \frac{\sum_{i=0}^{T} in_i}{\sum_{i=0}^{T} n_i}, \tag{8}$$

and

$$m_2 = \frac{\sum_{i=T+1}^{J_{max}(x,y)} in_i}{\sum_{i=T+1}^{J_{max}(x,y)} n_i}. \tag{9}$$

The term i in (8) and (9) represents the intensity levels present in the de-noised image and n_i represents the number of occurrences of the pixels with the intensity value i in the image. Since here the target is to determine the final threshold value T_{th} based on the optimization function, thus the value of T for which the function given in (4) generate the lowest values is considered as the final threshold value. Thus, the final threshold value T_{th} is obtained by the equation as given in (10).

$$T_{th} = arg \min_{0 \le T \le J_{max}(x,y)} E(T). \tag{10}$$

Finally, the segmented de-noise image is given by;

$$I_s(x,y) = \begin{cases} 1 & \text{if } J(x,y) \ge T_{th} \\ 0 & \text{if } J(x,y) < T_{th}. \end{cases} \tag{11}$$

The proposed technique has been illustrated in Algorithm 1.

Algorithm 1 Proposed method.

Input: I
Initialization: $J = 0$, $I_s = 0$, $E_{th} = 1$, and other parameters
$A \longleftarrow W_{row}$, $B \longleftarrow W_{column}$
for $i = 1:1:M$ **do**
  for $j = 1:1:N$ **do**
    $I_{reshape} \longleftarrow I(i-A:i+A, j-B:i+B)$
    $I_{max} \longleftarrow max(I_{reshape})$
    $I_{min} \longleftarrow min(I_{reshape})$
    $I_{med} \longleftarrow median(I_{reshape})$
    Calculate $J(i,j)$ using (2)
$D \longleftarrow max(J) - min(J)$
$T = min(J)$
for $T < max(J)$ **do**
  Calculate m_1 and m_2 using (8) and (9) respectively
  Calculate μ_J using (6)
  Calculate Shannon's entropy using $S_e = -\mu_j ln\mu_j - (1-\mu_j)ln(1-\mu_j)$
  Calculate energy function $E(T)$ for threshold level T using (4)
  $T \longleftarrow T+1$
$E_{min} \longleftarrow min(E)$
$T \longleftarrow min(J)$
for $T < max(J)$ **do**
  if $E(T) = E_{min}$ **then**
    $T_{th} \longleftarrow T$
    break;
  else
    $T_{th} \longleftarrow T$
  $T \longleftarrow T+1$
Output: $I_s \longleftarrow J \ge T_{th}$.

4 Results and discussions

The proposed FFFT technique has been tested on ten different types of examples (Fig. 1). Zero mean Gaussian noise with systematically increased σ (standard deviation) has been induced in the original images. The corresponding outcome obtained after applying the proposed technique has been compared with other state-of-the-art methodologies and a few heuristically developed methods, in terms of both visual and quantitative analysis. The corresponding noisy images with different σ values have been shown in the first row of Figs. 2, 3, 4, 5, 6, 7, 8, 9, 10, 11, 12, 13, 14, 15, 16, 17, 18, 19, 20, 21, 22, 23, 24, 25, 26, 27, 28, 29, 30 and 31 respectively.

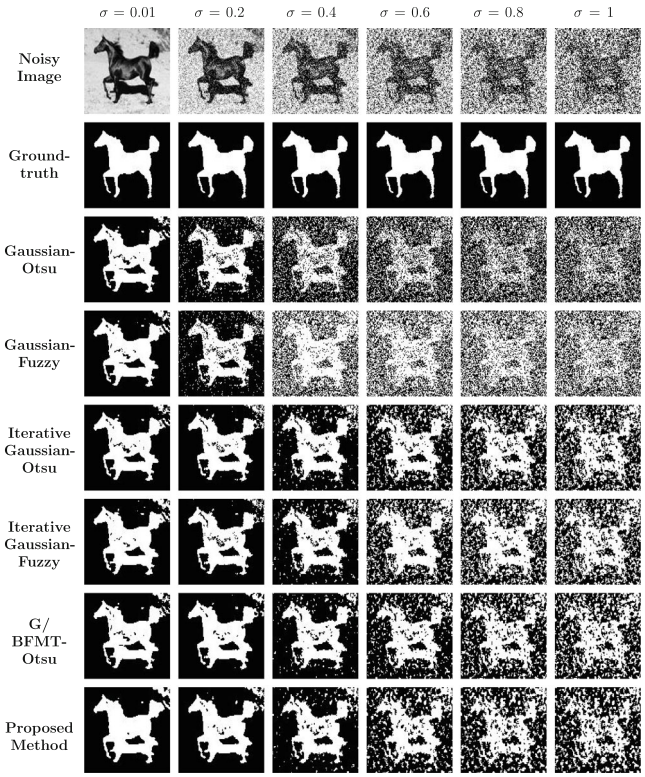

Fig. 10 Visual comparison between Gaussian based methods and proposed method for image *horse2*

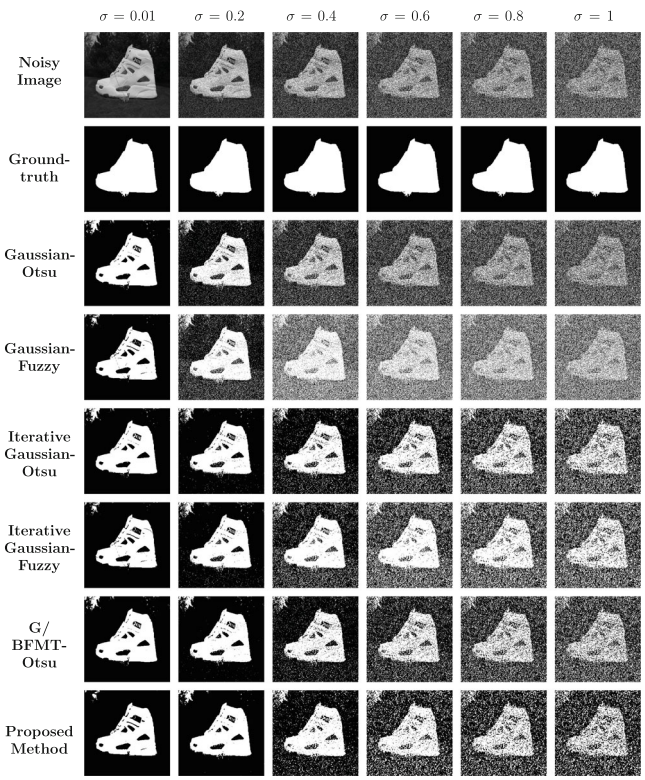

Fig. 11 Visual comparison between Gaussian based methods and proposed method for image *shoe*

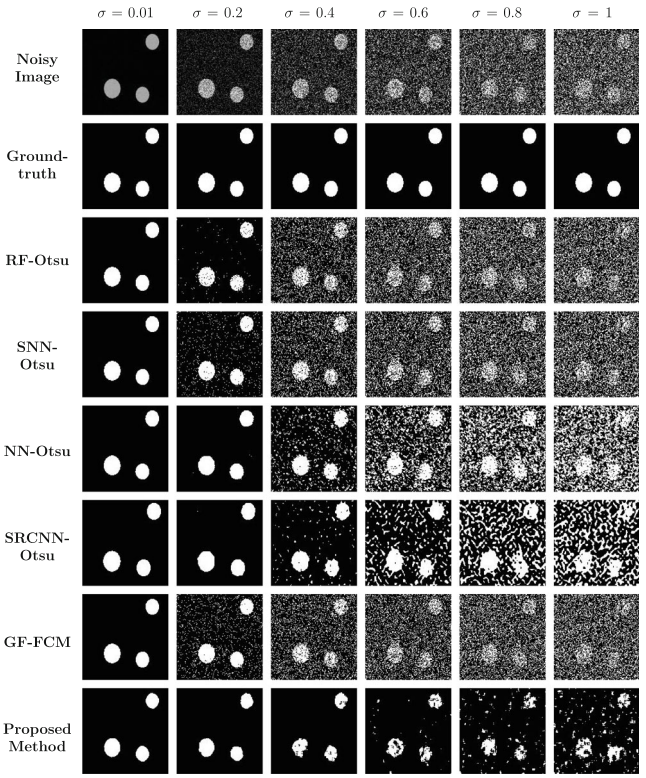

Fig. 12 Visual comparison between ML based algorithms and proposed method for image *c3*

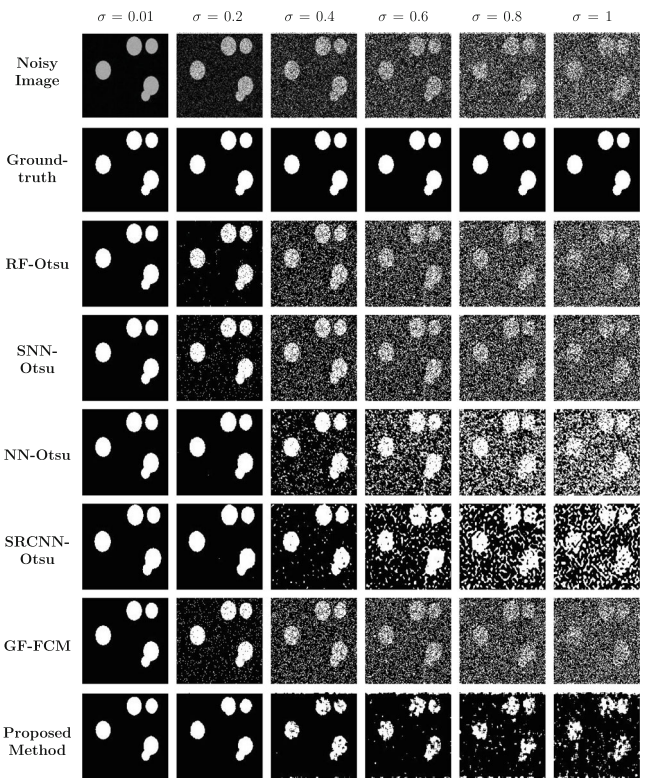

Fig. 13 Visual comparison between ML based algorithms and proposed method for image *c4*

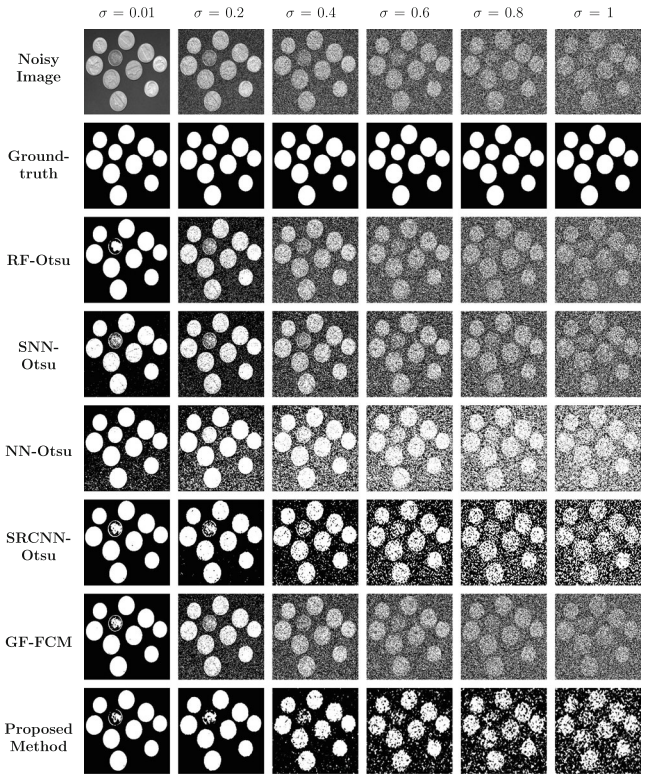

Fig. 14 Visual comparison between ML based algorithms and proposed method for image *coins*

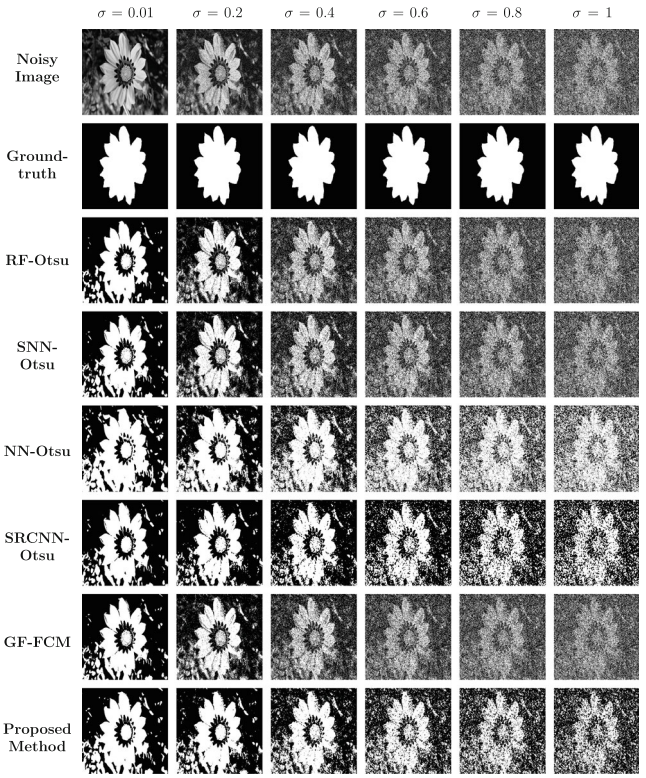

Fig. 16 Visual comparison between ML based algorithms and proposed method for image *sunflower*

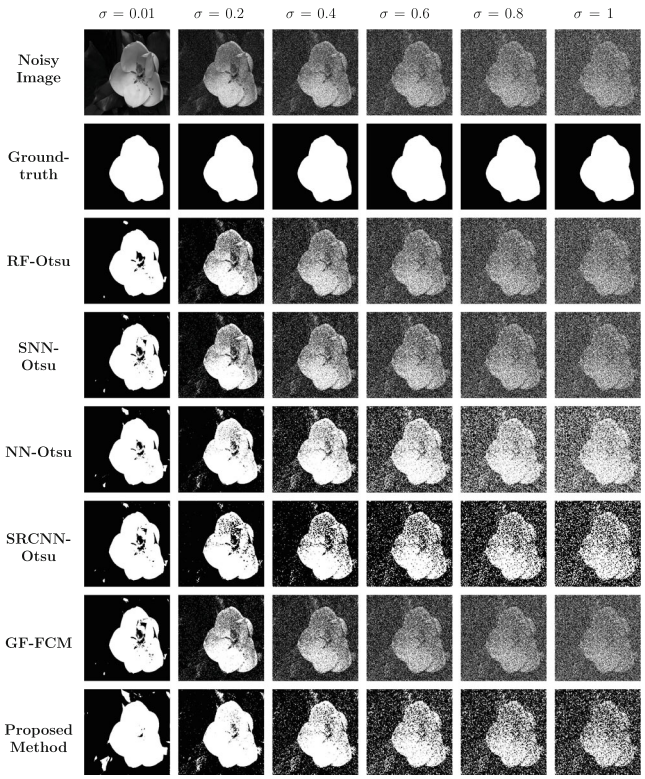

Fig. 15 Visual comparison between ML based algorithms and proposed method for image *flower*

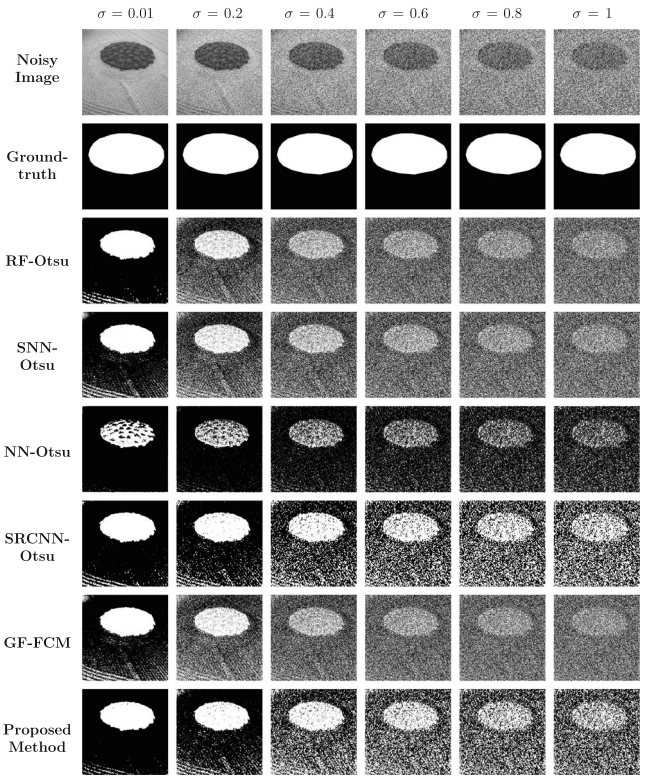

Fig. 17 Visual comparison between ML based algorithms and proposed method for image *cell*

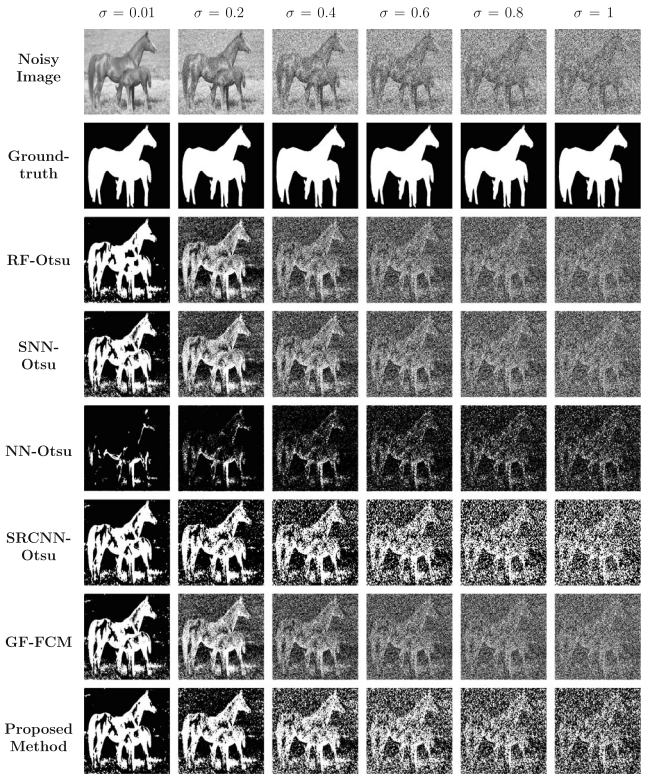

Fig. 18 Visual comparison between ML based algorithms and proposed method for image *horse1*

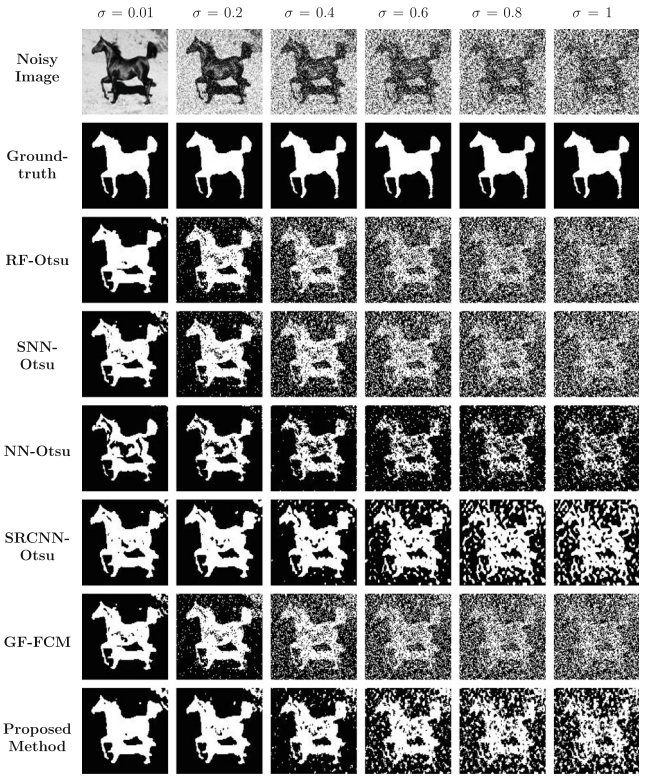

Fig. 20 Visual comparison between ML based algorithms and proposed method for image *horse2*

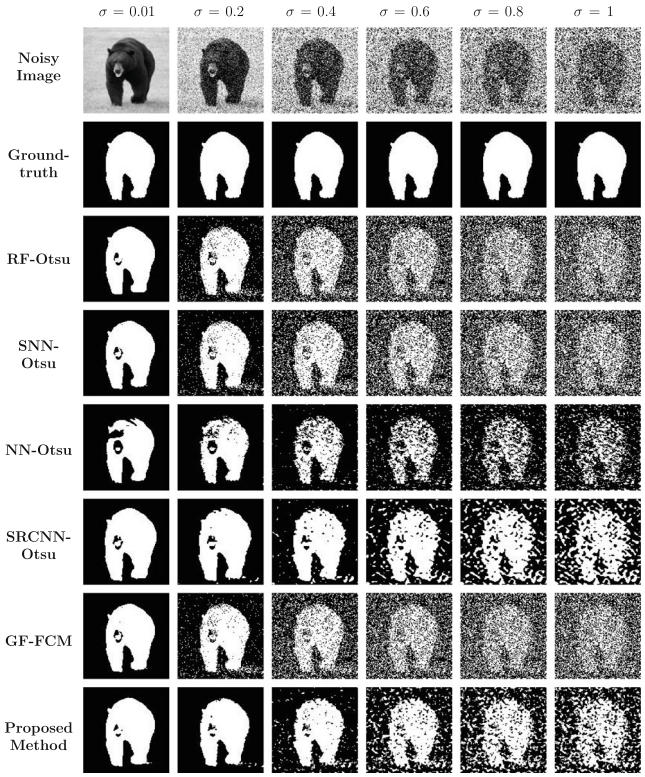

Fig. 19 Visual comparison between ML based algorithms and proposed method for image *bear*

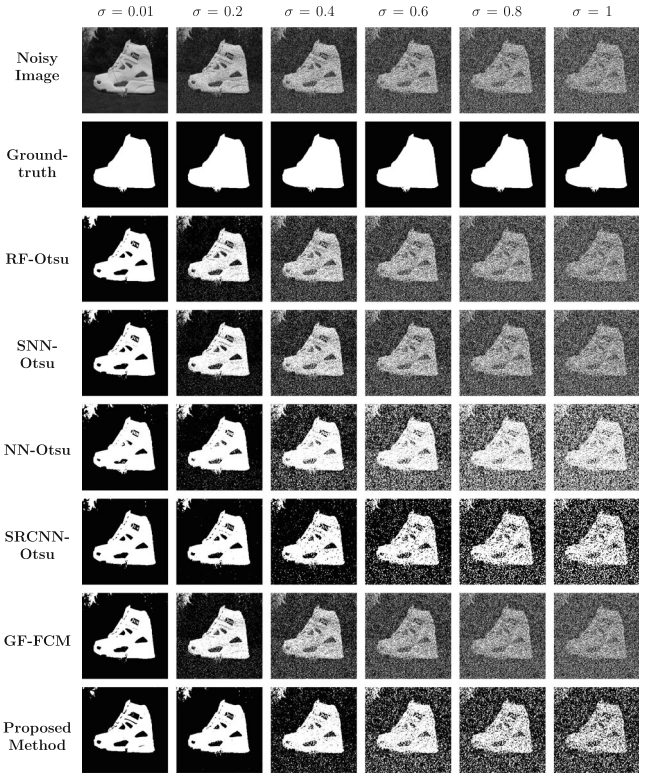

Fig. 21 Visual comparison between ML based algorithms and proposed method for image *shoe*

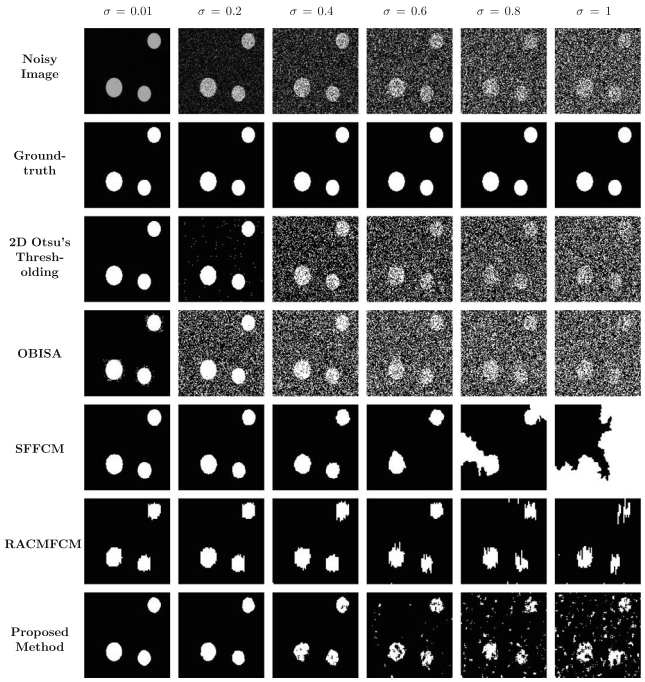

Fig. 22 Visual comparison between direct segmentation based algorithms and proposed method for image *c3*

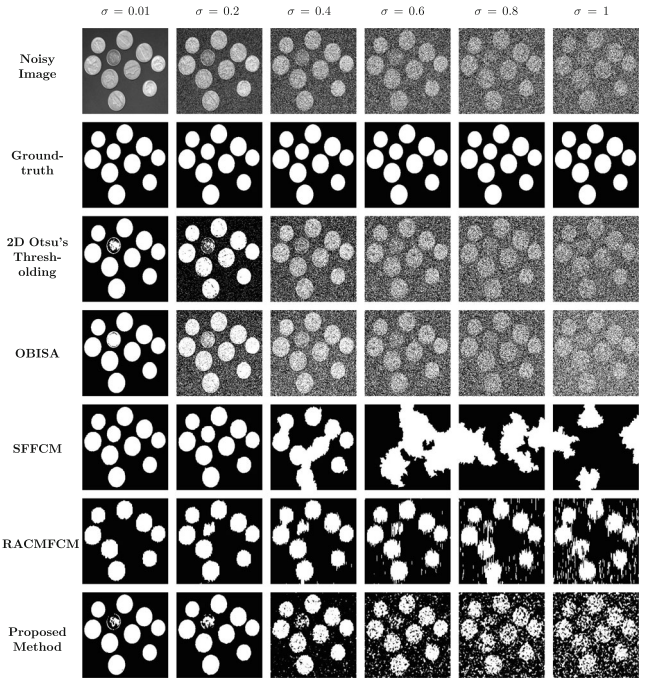

Fig. 24 Visual comparison between direct segmentation based algorithms and proposed method for image *coins*

4.1 Dataset

Dataset used for testing and validating the proposed method has been collected from MSRA10K Salient Object Database,[1] the DUT-OMRON Image Dataset,[2] Caltech-256 Object Category Dataset[3] and image co-segmentation dataset.[4] The dataset used is shown in Fig. 1.

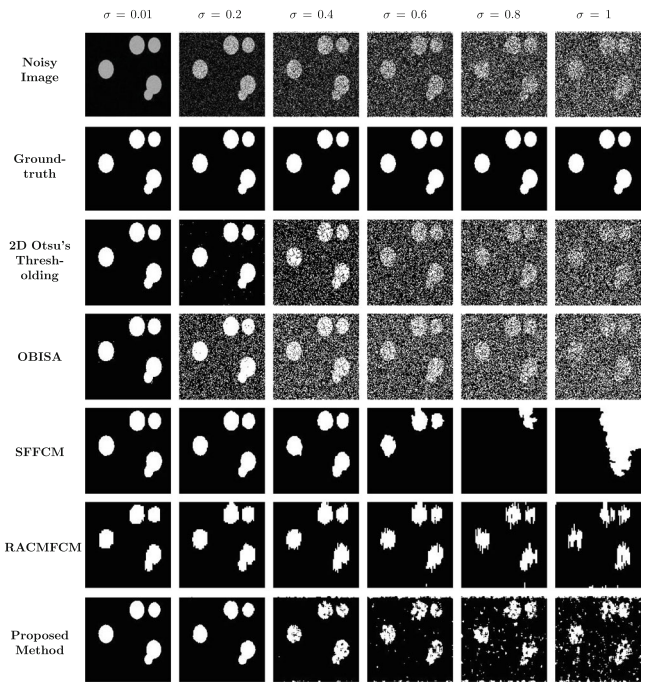

Fig. 23 Visual comparison between direct segmentation based algorithms and proposed method for image *c4*

Among the shown dataset, the first two examples are synthetic images. These two (Figs. 1a and b) are MATLAB generated image of *circles*. The image of the *coin* (shown in Fig. 1c) present in MATLAB built-in dataset have also been considered for the experimentation purpose.

The complexity of the data sets has been increased gradually. The first data *c3* in Fig. 1a, consists of three circles with a little variation of gray level intensity. Similarly, Figs. 1b contains 5 circles of different radius, along with two overlapping circles in each of them. The image Fig. 1c consists of a set of coins with a huge variation in the gray-scale level. The rest images in Fig. 1 are the color images. Images used for the experiment are having the maximum resolution of 400 × 320 *pixels*, while minimun image size used for the experiment is having resolution of 128 × 96 *pixels*.

4.2 Comparison methodologies

The proposed FFFT technique is compared with the other existing algorithms of object detection in a noisy image

[1] https://mmcheng.net/msra10k/

[2] http://saliencydetection.net/dut-omron/

[3] http://www.vision.caltech.edu/Image_Datasets/Caltech256/

[4] http://ivipc.uestc.edu.cn/project/FanmanMengSMCB/

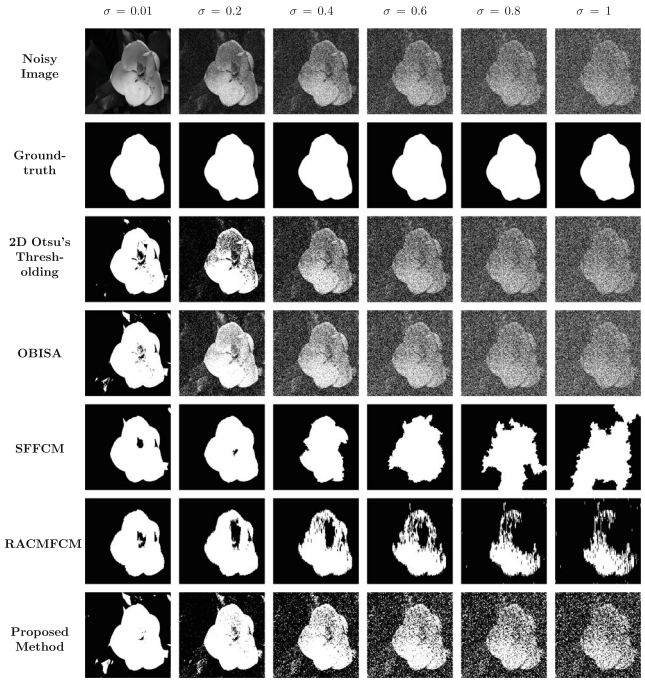

Fig. 25 Visual comparison between direct segmentation based algorithms and proposed method for image *flower*

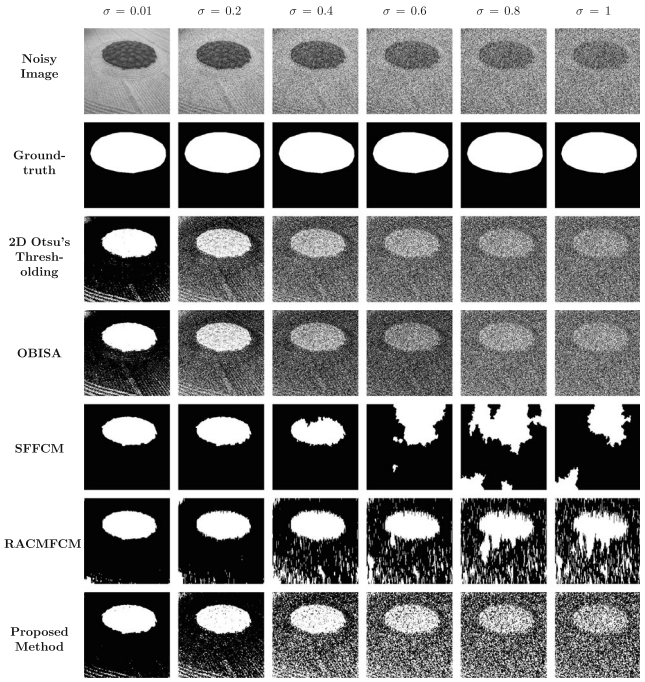

Fig. 27 Visual comparison between direct segmentation based algorithms and proposed method for image *cell*

as well as few heuristically developed methodologies. In heuristically developed methods, various combinations of newly developed de-noising techniques and state-of-the-art segmentation algorithms has been used for the comparison purpose.

Based on the noise removal and object extraction procedure, methodologies have been divided into three groups, namely; Gaussian filter based techniques, machine-learning (ML) based techniques and direct segmentation technique.

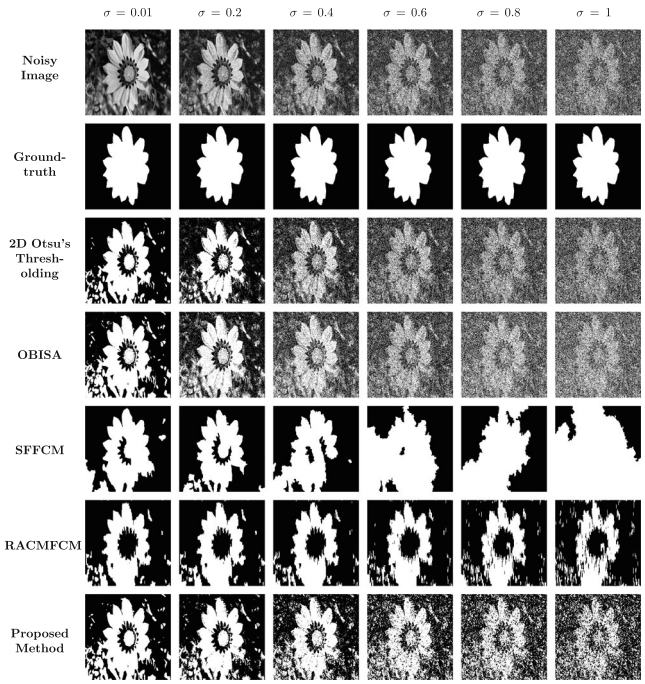

Fig. 26 Visual comparison between direct segmentation based algorithms and proposed method for image *sunflower*

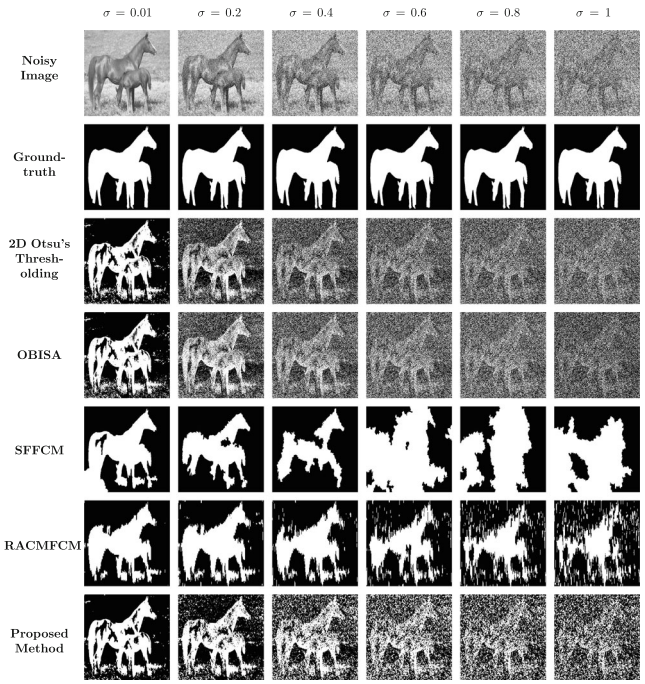

Fig. 28 Visual comparison between direct segmentation based algorithms and proposed method for image *horse1*

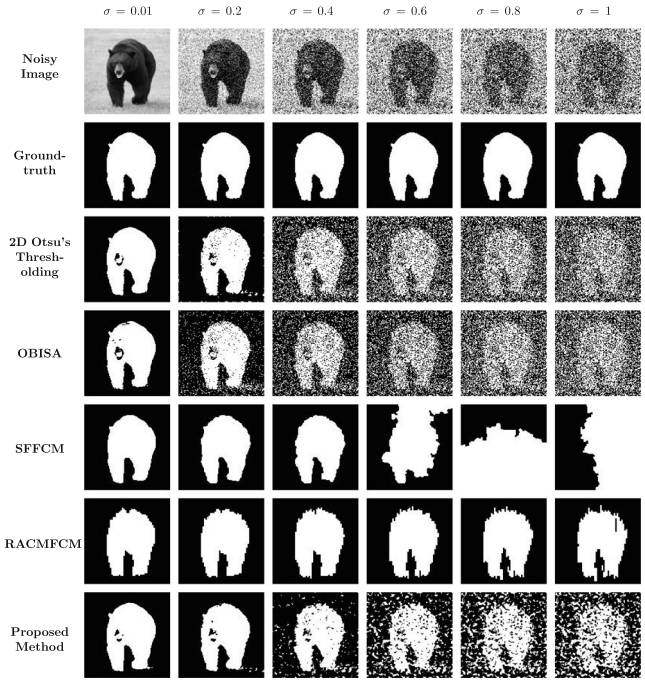

Fig. 29 Visual comparison between direct segmentation based algorithms and proposed method for image *bear*

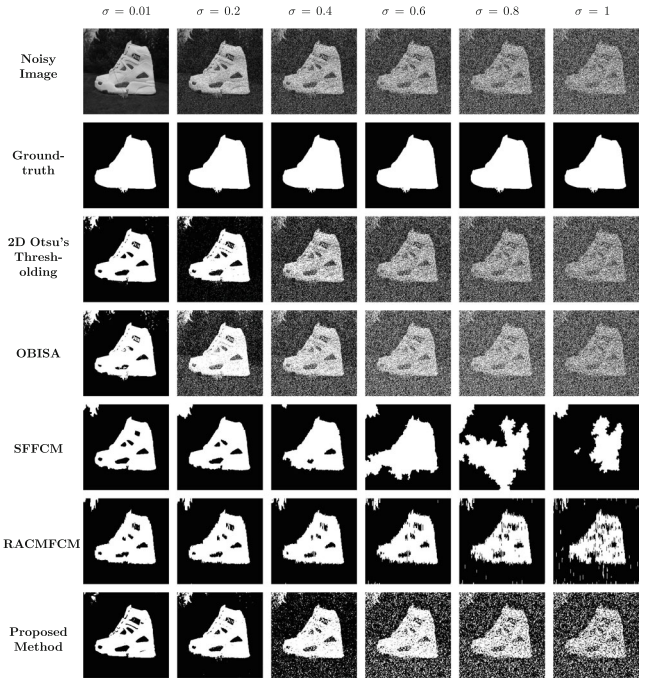

Fig. 31 Visual comparison between direct segmentation based algorithms and proposed method for image *shoe*

The Gaussian-based techniques explicitly incorporate Gaussian function in the process of noise removal followed by Otsu's or fuzzy thresholding. Following combinations are formed, (1) Gaussian noise filtering and Otsu's thresholding method (Gaussian-Otsu), (2) Gaussian noise filtering and fuzzy thresholding method (Gaussian-Fuzzy), (3) Iterative Gaussian noise filtering and Otsu's thresholding method (Iterative Gaussian-Otsu), (4) Iterative Gaussian noise filtering and fuzzy thresholding method (Iterative Gaussian-Fuzzy) and (5) G/BFMT and Otsu's thresholding technique (G/BFMT-Otsu).

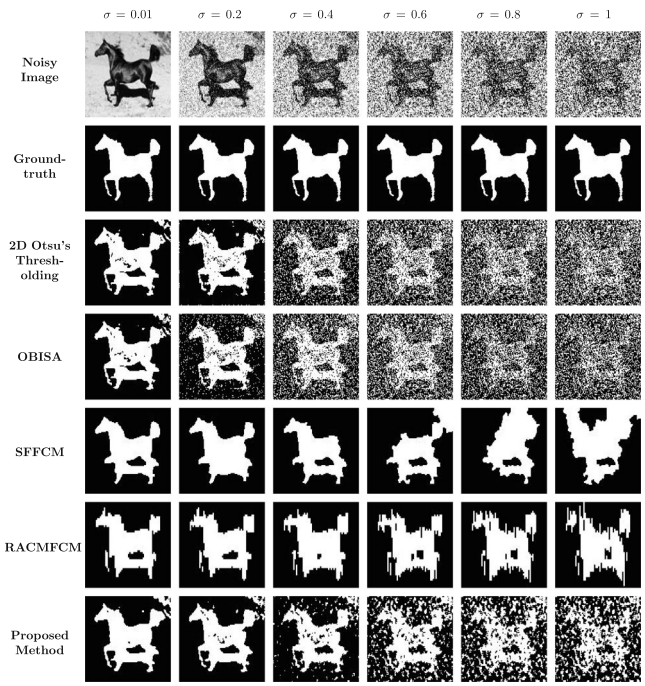

Fig. 30 Visual comparison between direct segmentation based algorithms and proposed method for image *horse2*

On the other-hand. (1) RF and Otsu's thresholding (RF-Otsu), (2) SNN and Otsu's thresholding (SNN-Otsu), (3) NN and Otsu's thresholding (NN-Otsu), (4) SRCNN and Otsu's thresholding (SRCNN-Otsu) and, (5) guided filter and fuzzy clustering (GF-FCM) have been classified into ML based technique.

In addition, methods which directly operate on the noisy image and segment out the RoI, such as (5) 2D Otsu's thresholding, (6) SFFCM, (7) OBISA and (6) RACMFCM have been included in third group.

4.3 Visual analysis

The results are shown in Figs. 2–31. In the Figs. 2–31, the first row indicates the original noisy images obtained for different σ values and the very next row contains the corresponding ground-truth images. The last row shows the outputs obtained using the proposed technique. The results generated using other methods have been shown in between the second and last rows of the figures.

Comparisons with Gaussian filter based techniques have been shown in the Figs. 2–11, machine learning based

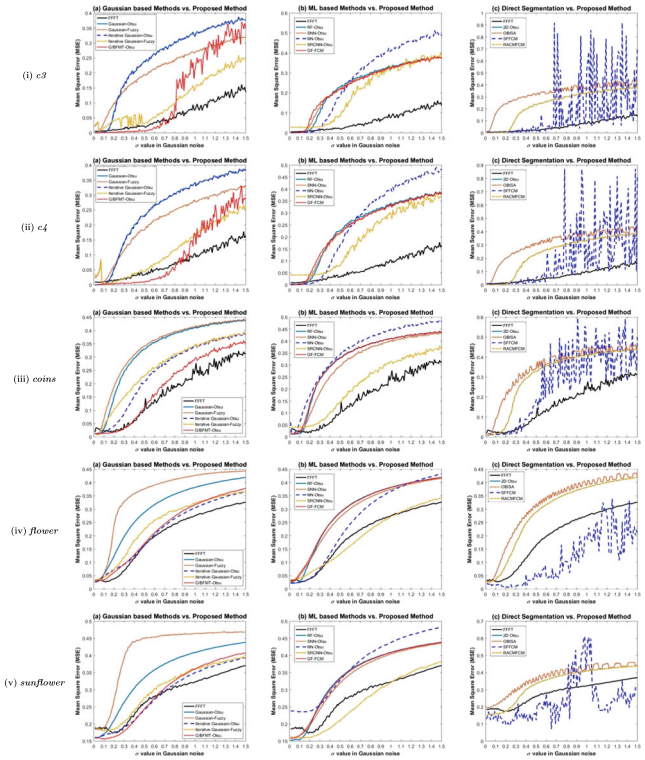

Fig. 32 MSE graph of output obtained using different methods for different values of σ and ${\sigma_{IN}}^2$ for mentioned images

techniques have been shown in Figs. 12–21 and Figs. 22–31 indicates the results obtained from direct segmentation techniques.

From the figures, it can be seen that the proposed technique is showing promising performance in object detection in presence of high amount of Gaussian noise. Only iterative Gaussian with fuzzy thresholding shows similar performance to that of the proposed technique in presence of high noise.

The figure indicates the important role of noise removal in accurate object detection as both fuzzy and Otsu perform similar way while Gaussian filtering is used. However, fuzzy based segmentation performs much better than Otsu's method when the iterative Gaussian filter is used to remove the noise. The fuzzy method able to extract the useful information from de-noised image withstanding the significant blurring effect due to multiple iterations.

The proposed FFFT technique has segmented out most part of the objects from noisy image better compared to the other discussed methods. The main reason behind this is the combined advantage of ATFFMED and fuzzy thresholding. The first helps in eliminating the noise from the image while retaining the maximum details and, the second one helps in generating the segmented output by reducing the misclassification probability using fuzzy membership function. From the images shown Figs. 22-31, it can be noted that RACMFCM method is also show good results in extraction of RoI from noisy images. However, it can also be noted from Figs. 32 and 33 that RACMFCM technique performs poorer than the proposed techniques for some of the images. The main reasons behind this mis-classification are; first, the performance of the method in detecting RoI depends on contour initialization, and second, the evolution of contour in this method depends on mean values of foreground and background pixels initially generated using FCM,and does not change for rest of the iteration.

4.4 Quantitative analysis

The results have also been compared quantitatively for verifying the performance of the proposed technique. Performance of the proposed technique, the existing methods and heuristically developed techniques have been measured in terms of PSNR and MSE for different values of σ and corresponding total image variance after addition of noise ${\sigma_{IN}}^2$; where the MSE and PSNR have been calculated by the equations given in (12) and (13) respectively.

$$MSE = \frac{\sum_{x=0}^{M}\sum_{y=0}^{N}\left[I_g(x,y) - I_s(x,y)\right]^2}{M \times N}, \tag{12}$$

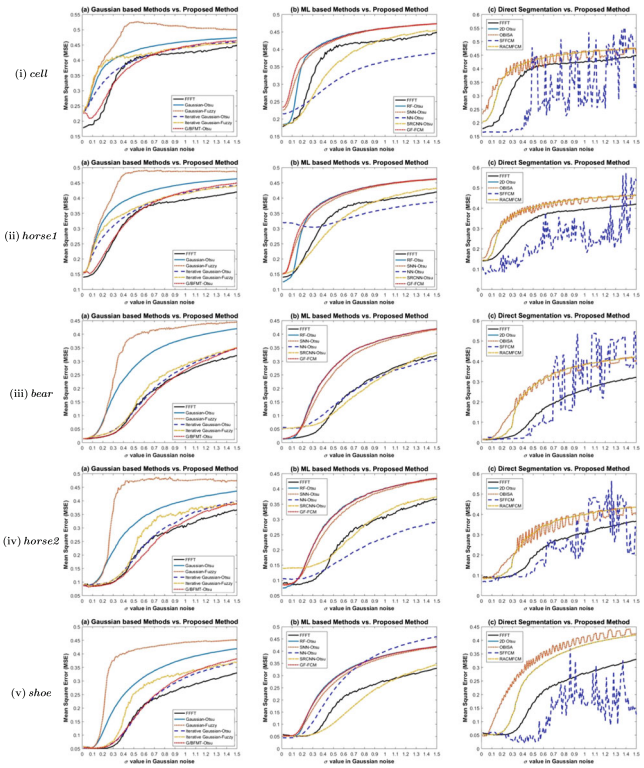

Fig. 33 MSE graph of output obtained using different methods for different values of σ and ${\sigma_{IN}}^2$ for mentioned images

Table 1 PSNR and MSE value of the de-noised output of *coin* image obtained using gaussian based techniques and proposed method for different values of σ and ${\sigma_{IN}}^2$

Methods	Measurement metrics	Sigma value /Total image variance					
		$\sigma = 0.01$ / ${\sigma_{IN}}^2 = 3788.249$	$\sigma = 0.2$ / ${\sigma_{IN}}^2 = 5002.877$	$\sigma = 0.4$ / ${\sigma_{IN}}^2 = 7435.233$	$\sigma = 0.6$ / ${\sigma_{IN}}^2 = 9354.411$	$\sigma = 0.8$ / ${\sigma_{IN}}^2 = 10661.975$	$\sigma = 1$ / ${\sigma_{IN}}^2 = 11506.566$
Gaussian-Otsu	MSE	0.0308672	0.1521680	0.2964499	0.3555691	0.3887534	0.4098916
	PSNR (in dB)	63.270	56.342	53.445	52.656	52.268	52.038
Gaussian-Fuzzy	MSE	0.0311789	0.1893360	0.3098238	0.3632249	0.3935501	0.4138076
	PSNR (in dB)	63.226	55.392	53.254	52.563	52.215	51.997
Iterative Gaussian-Otsu	MSE	0.0190108	0.0417344	0.1565989	0.2466396	0.3003930	0.3395393
	PSNR (in dB)	65.375	61.960	56.217	54.244	53.388	52.856
Iterative Gaussian-Fuzzy	MSE	0.0178591	0.1046477	0.1962466	0.2599051	0.3085366	0.3439837
	PSNR (in dB)	65.646	57.968	55.237	54.017	53.272	52.799
G/BFMT-Otsu	MSE	***0.0133740***	***0.0187534***	0.0671274	0.1589973	0.2375610	0.2947154
	PSNR (in dB)	***66.902***	***65.434***	59.896	56.151	54.407	53.471
Proposed Method	MSE	0.0152168	0.0233198	***0.0616531***	***0.1408808***	***0.1847696***	***0.2527507***
	PSNR (in dB)	66.342	64.488	***60.265***	***56.676***	***55.498***	***54.138***

Table 2 PSNR and MSE value of the de-noised output of *coin* image obtained using machine-learning based methods and proposed method for different values of σ and ${\sigma_{IN}}^2$

Methods	Measurement Metrics	Sigma value /Total image variance					
		$\sigma = 0.01$ / ${\sigma_{IN}}^2 = 3788.249$	$\sigma = 0.2$ / ${\sigma_{IN}}^2 = 5002.877$	$\sigma = 0.4$ / ${\sigma_{IN}}^2 = 7435.233$	$\sigma = 0.6$ / ${\sigma_{IN}}^2 = 9354.411$	$\sigma = 0.8$ / ${\sigma_{IN}}^2 = 10661.975$	$\sigma = 1$ / ${\sigma_{IN}}^2 = 11506.566$
RF-Otsu	MSE	0.0143631	0.1289566	0.2957859	0.3563686	0.3892818	0.4106233
	PSNR (in dB)	66.592	57.060	53.455	52.646	52.262	52.030
SNN-Otsu	MSE	0.0216260	0.0938618	0.2544986	0.3269377	0.3741463	0.4002168
	PSNR (in dB)	64.815	58.440	54.108	53.020	52.434	52.142
NN-Otsu	MSE	0.0613550	0.1728049	0.3031978	0.3734959	0.4184959	0.4495664
	PSNR (in dB)	60.286	55.789	53.348	52.442	51.948	51.637
SRCNN-Otsu	MSE	0.0409485	0.0465447	0.1011382	0.1915989	0.2681843	0.3152439
	PSNR (in dB)	62.042	61.486	58.116	55.341	53.880	53.178
GF-FCM	MSE	***0.0122493***	0.1424661	0.2934417	0.3551355	0.3883198	0.4102168
	PSNR (in dB)	***67.284***	56.628	53.490	52.661	52.273	52.035
Proposed Method	MSE	0.0152168	***0.0233198***	***0.0616531***	***0.1408808***	***0.1847696***	***0.2527507***
	PSNR (in dB)	66.342	***64.488***	***60.265***	***56.676***	***55.498***	***54.138***

Table 3 PSNR and MSE value of the de-noised output of *coin* image obtained using direct segmentation methods and proposed method for different values of σ and ${\sigma_{IN}}^2$

Methods	Measurement Metrics	Sigma value /Total image variance					
		$\sigma = 0.01$ / ${\sigma_{IN}}^2 = 3788.249$	$\sigma = 0.2$ / ${\sigma_{IN}}^2 = 5002.877$	$\sigma = 0.4$ / ${\sigma_{IN}}^2 = 7435.233$	$\sigma = 0.6$ / ${\sigma_{IN}}^2 = 9354.411$	$\sigma = 0.8$ / ${\sigma_{IN}}^2 = 10661.975$	$\sigma = 1$ / ${\sigma_{IN}}^2 = 11506.566$
2D Otsu's Thresholding [30]	MSE	0.0163550	0.0555014	0.2940244	0.3567209	0.3893767	0.4096477
	PSNR (in dB)	66.028	60.722	53.481	52.642	52.261	52.041
OBISA	MSE	***0.0074526***	0.2164228	0.3382927	0.3640786	0.3946206	0.4497290
	PSNR (in dB)	***69.442***	54.812	52.872	52.553	52.203	51.635
SFFCM [39]	MSE	0.0125474	***0.0128726***	0.0878049	0.2936314	0.2894173	0.3081436
	PSNR (in dB)	67.179	***67.068***	58.730	53.487	53.550	53.277
RACMFCM	MSE	0.0749593	0.0630081	0.0738482	***0.0868835***	***0.1240650***	***0.1644715***
	PSNR (in dB)	59.417	60.171	59.481	***58.775***	***57.228***	***56.004***
Proposed Method	MSE	0.0152168	0.0233198	***0.0616531***	0.1408808	0.1847696	0.2527507
	PSNR (in dB)	66.342	64.488	***60.265***	56.676	55.498	54.138

$$PSNR = 10log_{10}\frac{M_{FL}^2}{MSE}, \tag{13}$$

In the above (12) the term $I_g(x, y)$ denotes original ground-truth image. The segmented de-noised image has been compared with ground truth to generate MSE value. And the term M_{FL} indicates the maximum fluctuation level present in the image. For this case, its value has been considered -3 equal to 255 as the ground-truth images are 8-bit images.

As an example, the MSE and PSNR values obtained for different de-noised object detection algorithms is given in Tables 1, 2 and 3 for de-noised *coin* image, where bold symbol indicates the methods having the lowest MSE and PSNR values for a particular value of standard deviation. The comparisons of the proposed technique with other algorithms have been shown in Figs. 32 and 33.

From the Figs. 32iii–a and iii–b and the data stated in Tables 1 and 2, it can be concluded that the proposed technique shows lower MSE value for the noisy images with high σ values in comparison to other heuristically developed techniques and ML based techniques. This fact also holds true for the other cases as well as shown in Figs. 32 and 33. However, it should be noted that some of the existing techniques as well as heuristically developed methods performs better than the proposed techniques for specific images, such as NN-Otsu performs better in case of *horse2* while SFFCM performs better in case of images like *flower*, *sunflower* and *horse2*. The G/BFMT-Otsu technique is also found to perform better than the FFFT technique for low σ values at some of the images. In other cases the performances of the proposed model are similar or better to the other existing as well as heuristically developed methods for low σ values as well. The possible reason for obtaining better results in SFFCM than proposed technique is due to the presence of single object in the image. The performance of proposed technique is always higher than SFFCM when the image contains multiple objects. The performance of NN-Otsu, however, depends strongly on the training dataset. Since the same trained network is used in all of the study cases, the good performances in only in few cases indicate this fact. This is, in fact, one of the major issues in any neural network based algorithms. The performance of G/BFMT-Otsu depends on the variance of the filter as well as pixel intensity in image, hence perform better than the proposed technique only for low noise cases. The parameter tuning is one of the important aspect of this method. On the other hand, though the performance of RACMFCM is good in comparison to the proposed technique, it requires manual intervention in initializing the contours. Considering the fact that the proposed FFFT technique does not require human interaction (like in contour based method), or parameter tuning (like in Gaussian filters) as well no a-priory knowledge of the noise (like in NN based techniques), the results are quite satisfactory.

5 Conclusions

The work proposed a hybrid fuzzy filtering and fuzzy thresholding (FFFT) technique in detection and extraction of the object present in the noisy image. The technique is fully automated and no human interaction is required as in case of contour based technique. The output obtained using the proposed technique have been compared with other existing algorithms and heuristically developed algorithms for eight test images with varied level of σ values. It can be concluded that the proposed technique is capable of generating better output with high PSNR value and low MSE rate for Gaussian noise with high values of standard deviation compared to the most of the stated algorithms. Moreover, the method does not require the parameter tuning like Gaussian based techniques and prior information like neural network based methodologies for detection of RoI. However, it has been found that the algorithm results in high MSE rate for the low values of σ. In the future work, it will be in focus to handle this very limitation of the proposed technique. Applying the proposed algorithm on more realistic images such as remote sensing images, medical images, and astronomical images will be in the target for future work.

Acknowledgements The financial support received under DST INSPIRE Faculty grant is thankfully acknowledged.

References

1. Amza C (2012) A review on neural network-based image segmentation techniques
2. Baldwin JF, Karale SB (2003) Asymmetric triangular fuzzy sets for classification models. In: Palade V, Howlett RJ, Jain L (eds) Knowledge-based intelligent information and engineering systems. Springer, Berlin, pp 364-370
3. Bezdek JC, Ehrlich R, Full W (1984) Fcm: the fuzzy c-means clustering algorithm. Comput Geosci 10(2):191–203
4. Bhattacharyya S (2011) A brief survey of color image preprocessing and segmentation techniques. Journal of Pattern Recognition Research 1(1):120–129
5. Boukerma H, Choisy C, Farah N, Cheriet M (2018) The efficiency of the nshpz-hmm: theoretical and practical study. Appl Intell 48(12):4660–4677. https://doi.org/10.1007/s10489-018-1217-z
6. Boyat AK, Joshi BK (2014) Image denoising using wavelet transform and wiener filter based on log energy distribution over poisson-gaussian noise model. In: 2014 IEEE international conference on computational intelligence and computing research, pp 1–6
7. Buades A, Coll B, Morel JM (2005) Image denoising by non-local averaging. In: Proceedings. (ICASSP'05). IEEE international conference on acoustics, speech, and signal processing, 2005, vol 2, pp ii/25–ii/28. https://doi.org/10.1109/ICASSP.2005.1415332
8. Buades A, Coll B, Morel JM (2011) Non-local means denoising. Image Processing on Line 1:208–212. https://doi.org/10.5201/ipol.2011.bcm_nlm
9. Chen B, Huang S, Liang Z, Chen W, Pan B (2019) A fractional order derivative based active contour model for inhomogeneous image segmentation. Appl Math Modell 65:120–136. https://doi.org/10.1016/j.apm.2018.08.009. http://www.sciencedirect.com/science/article/pii/S0307904X18303986
10. Chi Y, Chan SH (2018) Fast and robust recursive filter for image denoising. In: 2018 IEEE international conference on acoustics, speech and signal processing (ICASSP), pp 1708–1712
11. Ciecholewski M (2015) Automated coronal hole segmentation from solar euv images using the watershed transform. J Vis Commun Image Represent 33:203–218
12. Citrin S, Azimi-Sadjadi MR (1992) A full-plane block kalman filter for image restoration. IEEE Trans Image Process 1(4):488–495
13. Dabov K, Foi A, Katkovnik V, Egiazarian K (2007) Image denoising by sparse 3-d transform-domain collaborative filtering. IEEE Trans Image Process 16(8):2080–2095. https://doi.org/10.1109/TIP.2007.901238
14. Danielyan A, Vehvilainen M, Foi A, Katkovnik V, Egiazarian K (2009) Cross-color bm3d filtering of noisy raw data. In: 2009 international workshop on local and non-local approximation in image processing. IEEE, pp 125–129
15. Dave RN (1991) Characterization and detection of noise in clustering. Pattern Recogn Lett 12(11):657–664
16. Deng G, Cahill LW (1993) An adaptive gaussian filter for noise reduction and edge detection. In: 1993 IEEE conference record nuclear science symposium and medical imaging conference, vol 3, pp 1615–1619
17. Dhanachandra N, Manglem K, Chanu YJ (2015) Image segmentation using k -means clustering algorithm and subtractive clustering algorithm. Prog Comput Sci 54:764–771. Eleventh international conference on image and signal processing
18. Dong C, Loy CC, He K, Tang X (2016) Image super-resolution using deep convolutional networks. IEEE Trans Pattern Anal Mach Intell 38(2):295–307
19. Elyor K, Lee G (2013) Automatic object segmentation using mean shift and growcut. In: The 19th Korea-Japan joint workshop on frontiers of computer vision, pp 184–189
20. Frosio I, Kautz J (2019) Statistical nearest neighbors for image denoising. IEEE Trans Image Process 28(2):723–738
21. George G, Oommen RM, Shelly S, Philipose SS, Varghese AM (2018) A survey on various median filtering techniques for removal of impulse noise from digital image. In: 2018 conference on emerging devices and smart systems (ICEDSS), pp 235–238. https://doi.org/10.1109/ICEDSS.2018.8544273
22. Getreuer P (2012) Chan-vese segmentation. Image Processing on Line 2:214–224
23. Ghosh P, Mali K, Das SK (2018) Chaotic firefly algorithm-based fuzzy c-means algorithm for segmentation of brain tissues in magnetic resonance images. J Vis Commun Image Represent 54:63–79
24. Guo L, Chen L, Chen CP, Zhou J (2018) Integrating guided filter into fuzzy clustering for noisy image segmentation. Digital Signal Processing 83:235–248. https://doi.org/10.1016/j.dsp.2018.08.022. http://www.sciencedirect.com/science/article/pii/S1051200418301465
25. Han B, Wu Y (2019) Active contours driven by global and local weighted signed pressure force for image segmentation. Pattern Recognit 88:715–728. https://doi.org/10.1016/j.patcog.2018.12.028. http://www.sciencedirect.com/science/article/pii/S0031320318304497
26. Chang H, Yeung D-Y, Xiong Y (2004) Super-resolution through neighbor embedding. In: Proceedings of the 2004 IEEE computer society conference on computer vision and pattern recognition,

2004. CVPR 2004, vol 1, pp I–I. https://doi.org/10.1109/CVPR.2004.1315043
27. Huang LK, Wang MJJ (1995) Image thresholding by minimizing the measures of fuzziness. Pattern Recogn 28(1):41–51
28. Jia H, Ma J, Song W (2019) Multilevel thresholding segmentation for color image using modified moth-flame optimization. IEEE Access 7:44,097–44,134. https://doi.org/10.1109/ACCESS.2019.2908718
29. Jia H, Peng X, Song W, Lang C, Xing Z, Sun K (2019) Hybrid multiverse optimization algorithm with gravitational search algorithm for multithreshold color image segmentation. IEEE Access 7:44,903–44,927. https://doi.org/10.1109/ACCESS.2019.2908653
30. Jianzhuang L, Wenqing L, Yupeng T (1991) Automatic thresholding of gray-level pictures using two-dimension otsu method. In: International conference on circuits and systems, vol 1, pp 325–327
31. Jin L (2017) Complex impulse noise removal from color images based on super pixel segmentation. J Vis Commun Image Represent 48:54–65
32. Jin R, Weng G (2019) A robust active contour model driven by fuzzy c-means energy for fast image segmentation. Digital Signal Processing 90:100–109. https://doi.org/10.1016/j.dsp.2019.04.004. http://www.sciencedirect.com/science/article/pii/S1051200418305451
33. Kalaimani G, Manojkumar K, Kumar SS (2019) Median filtering for removal of maximum impulse noise from images with a decision based model. J Comput Theor Nanosci 16(2):562–567
34. Kim KI, Kwon Y (2010) Single-image super-resolution using sparse regression and natural image prior. IEEE Trans Pattern Anal Mach Intell 32(6):1127–1133. https://doi.org/10.1109/TPAMI.2010.25
35. Ko S, Lee YH (1991) Center weighted median filters and their applications to image enhancement. IEEE Transactions on Circuits and Systems 38(9):984–993
36. Krinidis S, Chatzis V (2009) Fuzzy energy-based active contours. IEEE Trans Image Process 18(12):2747–2755
37. shiaw Kuo S, Johnston JD (2001) Spatial noise shaping based on human visual sensitivity and its application to image coding. In: Proceedings 2001 international conference on image processing (Cat. No.01CH37205), vol 2, pp 17–20
38. Kwan HK (2003) Fuzzy filters for noisy image filtering. In: Proceedings of the 2003 international symposium on circuits and systems, 2003. ISCAS '03, vol 4, pp IV–IV
39. Lei T, Jia X, Zhang Y, Liu S, Meng H, Nandi AK (2018) Superpixel-based fast fuzzy c-means clustering for color image segmentation. IEEE Trans Fuzzy Syst 27(9):1–1
40. Li Y, Cao G, Yu Q, Li X (2018) Active contours driven by non-local gaussian distribution fitting energy for image segmentation. Appl Intell 48(12):4855–4870. https://doi.org/10.1007/s10489-018-1243-x
41. Lowe DG (2004) Distinctive image features from scale-invariant keypoints. Int J Comput Vis 60(2):91–110. https://doi.org/10.1023/B:VISI.0000029664.99615.94
42. Mancas M, Gosselin B, Macq B (2005) Segmentation using a region-growing thresholding. In: Image processing: algorithms and systems IV, vol 5672, pp 388–399. International Society for Optics and Photonics
43. Morar A, Moldoveanu F, Gröller E (2012) Image segmentation based on active contours without edges. In: 2012 IEEE 8th international conference on intelligent computer communication and processing, pp 213–220
44. Mustafa WA, Yazid H (2016) Background correction using average filtering and gradient based thresholding. J Telecommunication Electr Comput Eng (JTEC) 8(5):81–88
45. Mustafa WA, Yazid H (2016) Illumination and contrast correction strategy using bilateral filtering and binarization comparison. J Telecommunication Electr Comput Eng (JTEC) 8(1):67–73
46. Mustafa WA, Yazid H, Yaacob SB (2014) Illumination normalization of non-uniform images based on double mean filtering. In: 2014 IEEE international conference on control system, computing and engineering (ICCSCE 2014), pp 366–371. https://doi.org/10.1109/ICCSCE.2014.7072746
47. Otsu N (1979) A threshold selection method from gray-level histograms. IEEE Trans Syst Man Cybern 9(1):62–66
48. Pal NR, Pal SK (1993) A review on image segmentation techniques. Pattern Recogn 26(9):1277–1294
49. Peng S, Lucke L (1994) Fuzzy filtering for mixed noise removal during image processing. In: Proceedings of 1994 IEEE 3rd international fuzzy systems conference, vol 1, pp 89–93
50. Sarker S, Chowdhury S, Laha S, Dey D (2012) Use of non-local means filter to denoise image corrupted by salt and pepper noise. Signal & Image Processing 3(2):223
51. Sha C, Hou J, Cui H (2016) A robust 2d otsu's thresholding method in image segmentation. J Vis Commun Image Represent 41:339–351
52. Shrestha S (2014) Image denoising using new adaptive based median filters. arXiv preprint arXiv:1410.2175
53. Shreyamsha Kumar BK (2013) Image denoising based on gaussian/bilateral filter and its method noise thresholding. SIViP 7(6):1159–1172. https://doi.org/10.1007/s11760-012-0372-7
54. Stein CM (1981) Estimation of the mean of a multivariate normal distribution. Ann Stat 9(6):1135–1151
55. Timofte R, De V, Gool LV (2013) Anchored neighborhood regression for fast example-based super-resolution. In: 2013 IEEE international conference on computer vision, pp 1920–1927. https://doi.org/10.1109/ICCV.2013.241
56. Timofte R, De Smet V, Van Gool L (2014) A+: adjusted anchored neighborhood regression for fast super-resolution. In: Asian conference on computer vision. Springer, pp 111–126
57. Trivedi MM, Bezdek JC (1986) Low-level segmentation of aerial images with fuzzy clustering. IEEE Trans Syst Man Cybern 16(4):589–598. https://doi.org/10.1109/TSMC.1986.289264
58. Turkmen I (2016) The ann based detector to remove random-valued impulse noise in images. J Vis Commun Image Represent 34:28–36
59. Unajan MC, Gerardo BD, Medina RP (2019) A modified otsu-based image segmentation algorithm (obisa). In: Proceedings of the international multiconference of engineers and computer scientists, pp 363–366
60. Ville DVD, Nachtegael M, der Weken DV, Kerre EE, Philips W, Lemahieu I (2003) Noise reduction by fuzzy image filtering. IEEE Trans Fuzzy Syst 11(4):429–436
61. Wang X, Wan Y, Li R, Wang J, Fang L (2016) A multi-object image segmentation c–v model based on region division and gradient guide. J Vis Commun Image Represent 39:100–106
62. Yang J, Wright J, Huang TS, Ma Y (2010) Image super-resolution via sparse representation. IEEE Trans Image Process 19(11):2861–2873. https://doi.org/10.1109/TIP.2010.2050625
63. Yu G, Sapiro G (2011) DCT image denoising: a simple and effective image denoising algorithm. Image Processing on Line 1:292–296. https://doi.org/10.5201/ipol.2011.ys-dct
64. Zhao F, Fan J, Liu H, Lan R, Chen CW (2019) Noise robust multiobjective evolutionary clustering image segmentation motivated by the intuitionistic fuzzy information. IEEE Trans Fuzzy Syst 27(2):387–401. https://doi.org/10.1109/TFUZZ.2018.2852289

Sanmoy Bandyopadhyay graduated in Electronics and Communication Engineering at Academy of Technology under West Bengal University of Technology (presently Maulana Abul Kalam Azad University of Technology) in 2009. In 2012, he received the M.Tech in same discipline with a major in Telecommunication Engineering from National Institute of Technology, Durgapur. Subsequently, he joined as a Research Fellow at the Center for Soft Computing Research, Indian Statistical Institute, Kolkata in 2012 and continued his work until 2018. He is currently pursuing his Ph.D. from IIT, Indore in the Discipline of Astronomy, Astrophysics and Space Engineering. He has authored or co-authored about 15 technical papers in journals, conference and book chapters and received best paper award for presenting paper in workshop organized by IEEE GRSS Kolkata Chapter. His research interests include antenna array synthesis, fuzzy logic and image processing. He serves as reviewer of several journals and conference proceedings. He is currently life member of Indian Science Congress and IEEE student member.

Saurabh Das received his Ph. D. in Radio Physics and Electronics from University of Calcutta, Kolkata, India, in 2013. He is currently working as an Assistant Professor at Discipline of Astronomy, Astrophysics and Space Engineering, IIT Indore. Earlier he worked as an faculty at Indian Statistical Institute and University of Calcutta and as a research fellow at Space Applications Centre, ISRO, Ahmedabad. His research interest includes radiowave propagation in atmosphere and ionosphere, radar meteorology, GNSS, and machine learning. He is a senior member of IEEE since 2017. He has published more than 25 papers in peer-reviewed journals and received young scientist awards in URSI 2014 and APRASC 2016.

Abhirup Datta received his Ph. D. in Physics (Astrophysics) from New Mexico Tech/NRAO, USA in February, 2011. He is currently working as an Associate Professor at Discipline of Astronomy, Astrophysics and Space Engineering, IIT Indore. He received the NASA Post-Doctoral Fellowship for the years 2011-2013. He was a senior Research Associate at University of Colorado, Boulder, USA. His research interests include observational cosmology, low-frequency radio and x-ray observations of Galaxy Clusters, Ionospheric effects on low frequency radio interferometric calibration and imaging, Space Weather, Sustainable Research and Big Data. He is a member of International Astronomical Union since 2018. He is also a member from India in the Square Kilometer Array (SKA) CD/EoR Science Team Board since January, 2017. He has published more than 30 papers in peer-reviewed journals.